nature portfolio

Peer Review File

Trigger inducible tertiary lymphoid structure formation using covalent organic frameworks for cancer immunotherapy

Corresponding Author: Professor Ben Zhong Tang

This file contains all reviewer reports in order by version, followed by all author rebuttals in order by version.

Version 0:

Reviewer comments:

Reviewer #1

(Remarks to the Author)
The authors propose an innovative approach to induce TLS in vivo for the purpose of treating established cancers in murine preclinical models of cancers. They leverage a novel covalent organic framework methodology and describe a mechanism of antitumor immunity at the single cell level. This work is highly interesting and they should be commended on their efforts.

Major
- Figure 1 is beautifully constructed but the legend incompletely explains elements in the figure (such as the CellphoneDB algorithm or the role of CTLA-4 inhibition or the primary and distant, presumably synchronous cancers).
- There are too many abbreviations - 18 in the first 2 pages alone! Needs to be addressed
- Fig 5 - on what day is the endpoint flow analysis conducted? It would be surprising to see Tcm early in the course of therapy. Would omit T cell changes in spleen - not clear how this relates to antitumor immunity in the TIME or tdLN.
- Fig 5 F - are the authors claiming that 60-70% of all CD45 cells in the tdLN are CD3 lymphocytes? This is inconsistent with published data for these well characterized preclinical models (and far outside of what is reasonably expected in a reactive tdLN during IO therapy)
- Fig 5 - necessary to explain how the DLN was defined
- Fig 6 - Would the authors expect that DCs be present in their TLS? were DCs below the 5% abundance threshold. If indeed below the 5% threshold, authors should strongly consider liberating this threshhold to capture these critical immune effectors - particulrly in light of the subsequent analysis exploring them by flow and the ELISA work showing significant elevations in CCL19 and CCL21. Please explain
- Fig 6 E - add statistics
- Fig 7 - where was 4MOSC1 injected for these experiments?
- Fig 7 b-d - excellent and convincing (Assuming that the modeling was orthotopic...)d
- Fig 8 - what was the tumor model here? add to fig legend and provide relevant methodology for tumor modeling and day of harvest (brief description would assist the reader here)
- Gating strategies in supp need have the decades added to the axes
- Supp Fig 15 - the gate for CD44 v CD62L looks to be inappropriately placed. The true CD44+ population looks to be at a higher decade than where the authors have placed the gate (as it is now, it looks to be bisecting the CD44- population)
- Fig 5 & Supp Fig 17 - would not expect MDSCs in the spleen in a preclinical tumor model. this should be addressed and explored in the TIME
- Supp 25 - need to add CXCL13 label to the figure
- Methods for in vitro/in vivo 4MOSC is needed
- Can the authors please comment and add a non-tumor model in vivo to convincingly demonstate that their TPDA-ViBT-COF+Laser does indeed lead to the minimal components and 3-D anatomy of recognized TLS. As is, only representative IF images are proposed for the readers to support TLS formation. Given that this work leverages a novel approach to induce TLS it is critical that ann independent, validated and well-used model is needed to convincingly demonstrate iTLS.
- Can the authors please provide data indicating the number of iTLS within tumors and the % volume of iTLS relative to total tumor volume. Do these analyses fit with what has been reported in the literature.
- The discussion is incomplete - need to add context for iTLS methodology and context for how the immuno-mechanistic findings with their iTLS fit into the existing literature. For example, the T cell infiltration data and ELISA with CCL19/CCL21 would suggest a critical role for DCs (as might be expected) but this is underexplored.

Minor
- references 5, 6, 12, 24 are not appropriately assigned to the corresponding claims in the text
- references Wang-Gutkind Nat Comm 2021 and Saddawi-Gutkind Nat Comm 2022 should be added to ref 64
- Please elaborate on how COFs and the formation of pearls relate. This is unclear and should be explained in the introduction with the appropriate reference. Additionally, if space allows, it should be explained concisely (briefly) in the abstract. It is clearly a feature of novelty that the authors have capitalized upon, but it is also very unfamiliar to the readers who will likely be attracted to this paper for its relation to antitumor immunity and IO and TLS.
- This sentence follows a claim regarding the limitation of TLS in cancer (below). It's an awkward transition and unclear how the concepts are connected. Re-writing is recommended.
- "Notably, the application of nanomedicines in cancer therapy has garnered significant attention owing to their excellent modifiability, targeting capability, functionality, and immune evasion properties.17-23"
- What's a MOF? not defined in introduction

Reviewer #2

(Remarks to the Author)
Zhang et al. present a well written article titled 'Trigger inducible tertiary lymphoid structure formation using covalent organic frameworks for cancer immunotherapy' in which they develop an artificial covalent organic framework for intra-tumor injection to induce tertiary lymphoid structure and anti-tumor immunity. The strength of this article is in optimizing this artificial nanostructure and its photothermal effects in inducing these effects. The article would be strengthened by addressing the following points:

- Tertiary lymphoid structures should be more clearly defined. In multiple areas in the article, the authors describe them as aggregrates of B cells interspersed with T cells. more peripherally CD31 vasculature presence in mentioned. Tertiary lymphoid structures generally require the full architecture of lymph nodes including high endothelial venules so better definition would be appreciated.

- In terms of models used, the authors selected a model in which other modalities have induced tertiary lymphoid structures. How is their methodology superior to other modalities previously tested that have induced TLS? For their second model they state they selected a model that is notable for its immune cell infiltration which I am presuming means high immune cell infiltration? Can they generate TLS in less immunogenic model as well?

- Figure 1 is dense but it is not clear what exactly it is showing. Better description in caption would be important.

- Figure 3. Abbreviations should be defined within figure/legend.

- Figure 5. Bar graphs are hazy and not bright in colors.

- Figure 6 shows cytokine secretion at bulk tumor level. Does single cell suggest what cells may be accounting for increased secretion of these?

- The authors state COF is associated with reduction in proportion of epithelial and stromal cells and that this suggests elimination of tumor and tumor fibroblast cells. It is instead possible that there is an increase in immune cell proportion due to inflammation but not necessarily elimination of other cell types but just relatively reduction in number as secondary effect.

- For discussion of scRNAseq, perhaps better phrasing that this suggests CTLA-4 blockade may be better partner than PD-1 blockade would be better rather than saying scRNAseq itself shows that CTLA-4 blockade 'exhibits synergistic effects'. Another part states 'conducted scRNAseq to investigate therapeutic efficacy of …in combination with different checkpoint blockade.' Would soften the language and rephrase.

- In discussion that PD-1 blockade may not be suitable given lower CD8 Tex on scRNAseq, as PD-1 blockade is also relevant in setting of myeloid cell PD-L1 expression, this should also be stated. Additionally I tis possible CTLA-4 displays higher expression in setting of T cell activation. Similarly the discussion on CD86 having higher expression with treatment is consistent with immune inflammation and activation. Overall the single cell rna sequencing support for why CTLA-4 rather than PD-1 blockade is not as convincing (in vivo data on other hand more supportive) so would perhaps rephrase.

- It would be helpful for discussion to include how this would be translated to patients which would presumably be intra-tumoral injection. How would this be activated by laser, etc?

- Given the authors are able to induce formation of these structures, it would be helpful to better understand which exact component is contributing to their formation if there is one? Is it a specific cytokine or specific immune cell type? Alternatively is it just general inflammation? What specifically about their structure is stimulating the required inflammation needed for TLS formation? In terms of therapeutic efficacy in their models, are the TLS contributing to response? Or simply a surrogate of the other immune effects and more a bystander?

Reviewer #3

(Remarks to the Author)

This manuscript has described a AIEgens-based covalent organic frameworks (COFs) with PDT and PTT therapeutic effects for the modulation of anti-tumour immune response. Utilizing the AIEgens-based COFs to promote the formation of tertiary lymphoid structures (TLS) to tune the anti-tumour immune response provides a new direction for future cancer immunotherapy. To further improve the quality of the manuscript for publication in Nature Communications, some concerns should be addressed.

1. In figure 4 f and l, how the authors decided the irradiation power and time?
2. The suitable particle size and water dispersity is one of the most important challenges for the application of COF as biomedical materials, thus, it would be more complete if the authors provide more information on the morphology related properties of COFs, such as size stability, size distribution of COFs in physiological environment.
3. As showed in figure 4 g, the TPDA-ViBT-COF showed an ellipse structure with a size of 180 nm, is the TPDA-TDTA-COF, TPDA-BT-COF showed a same size range and morphology, is there any relationship between the size, morphology and its PDT, PTT properties.
4. In figure 4, the authors showed excellent phototoxicity towards cancer cells, it would be more complete if the authors carry out more detailed studies on the phototoxicity on other cell types, such as immune cells, epithelial cells and stromal cells.
5. In supplementary fig 11, the authors showed the internalization of COFs into MC38 cells, it would be more complete if the authors can locate the subcellular organelle that the COFs in.
6. It would be more comprehensive if the authors carry out in vitro studies to show the activation of immune cells, such as maturation of DCs, polarization of macrophages as well as the proliferation and activation of T cells after treatment with AIE-COFs with cancer cells.
7. The biodistribution of COFs in tumour essentially its uptake by immune cells such as DCs, macrophages as well as T cells is an important question to answer considering the extreme cell cytotoxicity of COFs under laser irradiation. Thus, it would be more comprehensive if the authors can provide data on the distributions of COFs in tumours.
8. Why the authors choose intratumorally administration way? It would be more complete if the authors can carry out more studies on the impact of administration way of COFs on its therapeutic effects, such as i.v. injection.
9. As showed in figure 5, after treatment with COFs, including TPDA-TDTA-COF, TPDA-BT-COF, and TPDA-ViBT-COF showed a 30% to 70% complete tumour eradication. Besides, it showed a higher level of TCM and TEM, T, thus, it would be more complete if the authors can carry out a detailed tumour rechallenge studies.
10. In figure 5, the authors showed the changes on population of major immune cells in spleen and TDLN. It would be more direct if the authors carry out studies of the infiltration of immune cells inside the tumours as well as its activation.
11. In figure 6, the authors showed that, after treatment with COFs, the proportion of epithelial and stromal cell was sharply reduced, it would be more comprehensive if the authors can provide a possible explanation for such impact of COFs on those cells.
12. As showed in figure 6 e, after treatment with COFs, the proportion of Tregs was increased comparing with untreated group, why the PTT and PDT therapy have an impact on Tregs.?
13. Is there any difference on the PD-L1 expression on the tumours after treatment? why the combinational treatment with CTAL-4 antibody is better than PD-1 antibody?

Version 1:

Reviewer comments:

Reviewer #1

(Remarks to the Author)
Thank you for your detailed responses and the thoughtful revisions you've made in addressing my comments. I appreciate the effort to clarify and improve various aspects of your manuscript. Below are my thoughts on your responses:

Figure 1 Legend: The additional details provided in the figure legend significantly enhance the clarity. The explanation of the CellphoneDB algorithm and CTLA-4 inhibition is now clear and thorough. This revision is satisfactory.

Abbreviations: The inclusion of full names for abbreviations in the early sections of the manuscript addresses my concern about the text's readability. This change is appropriate and improves the manuscript's accessibility to a broader audience.

Fig 5 - Endpoint Flow Analysis: Your clarification regarding the timing of flow cytometry detection and the rationale behind including spleen data is well-explained. Including the updated data on T cells within the tumor strengthens this section. The revisions adequately address my concerns.

TDLN Definition: The clarification that "DLN" refers to "TDLN" and the corresponding revisions in the manuscript resolve the potential confusion. The added detail about the location of the TDLN in the context of your study is helpful and appropriate.

Fig 6 - DCs in TLS: Your efforts to validate the presence of dendritic cells in TLS using mIHC, along with the additional staining data, provide a convincing response to my comment. The explanation for the lack of DCs in scRNA-seq data is reasonable given the method's limitations. These additions have significantly strengthened your findings.

Fig 6E - Statistics: The addition of numerical descriptions and statistics to Fig 6E improves the rigor and interpretability of the data presented. This revision is satisfactory.

Tumor Model Clarification: The added description of the tumor models and methodology in the revised supplementary materials resolves my previous concern. Including these details makes the study more reproducible and transparent.

Gating Strategies: The inclusion of decades on the axes of the gating strategy figures in the Supplementary Materials addresses my comment appropriately. This addition improves the clarity and accuracy of your flow cytometry data.

TLS Formation in Non-Tumor Models: Your attempt to induce TLS in a non-tumor model and the subsequent findings add depth to your study. The explanation provided about the challenges of inducing TLS in non-tumor tissues is clear and addresses the comment satisfactorily.

iTLS Quantification: The quantification of iTLS within tumors and the discussion of the limitations related to TLS volume measurement are well-addressed. Your inclusion of this data adds valuable context to the manuscript.

Discussion on iTLS Methodology: The expanded discussion on iTLS methodology and its context within the existing literature enhances the manuscript's scientific discussion. The additional references to CCL19 and CCL21 in the context of dendritic cells and TLS formation are well-integrated.

References Assignment: The reassignment and addition of references as suggested aligns the citations more accurately with the corresponding claims. This revision is satisfactory.

COFs and Pearl Formation: The explanation of how COFs relate to the formation of pearls in the Introduction is a welcome addition. It connects the concept more clearly for readers unfamiliar with the field, making the novelty of your work more apparent.

Nanomedicine and TLS Induction: The rewritten section on nanomedicine's role in TLS induction is now more coherent and effectively links the concepts. The added definition of MOFs in the Introduction is also helpful for readers.

Overall, your revisions have addressed my comments comprehensively, and the manuscript is much improved as a result. I believe these changes have significantly strengthened your work, and I have no further major concerns. However, I encourage you to ensure that all statistical data is clearly presented, as consistent and transparent data presentation is crucial for maintaining scientific rigor.

Reviewer #2

(Remarks to the Author)
Zhang et al. re-submitted manuscript titled 'Trigger inducible tertiary lymphoid structure formation using covalent organic frameworks for cancer immunotherapy' in which they develop an artificial covalent organic framework for intra-tumor injection to induce tertiary lymphoid structure and anti-tumor immunity. The strength of this article is in optimizing this artificial nanostructure and its photothermal effects in inducing these effects. They have carefully and thoughtfully addressed the concerns expressed by myself as well as the other 2 reviewers to the best of their abilities. The figures and text read clearer with clearer descriptions and explanations of abbreviations. Required details on methodology and adjustment of flow analyses have also strengthened the manuscript. A few additional comments below:

1) Figure 7e - the labels on top PNAD, CD3, etc. don't seem to necessarily be in the same order in the single color stains below the multiplexed figure This should be corrected. This should be checked in all multiplexed figures.

2) Response to my 2nd comment on benefit of their methodology to induce TLS compared to others and limitations that it is not effective in cold tumors is significant. The inability to not induce in a cold tumor is a limitation in significance of this. It is not clear in their response that they included this in the manuscript and should include this limitation and discussion in the manuscript.

Reviewer #3

(Remarks to the Author)
This manuscript has described a AIEgens-based covalent organic frameworks (COFs) with PDT and PTT therapeutic effects for the modulation of anti-tumour immune response. Utilizing the AIEgens-based COFs to promote the formation of tertiary lymphoid structures (TLS) to tune the anti-tumour immune response provides a new direction for future cancer immunotherapy. To further improve the quality of the manuscript for publication in Nature Communications, some concerns should be addressed.

1. Several statements in the caption of figure1 should be further clarified, such as "the analysis indicated that αPD-1 expression in T cells….", "a ligand for αCTLA4".
2. In the revised manuscript, the authors showed that the AIE-COFs showed a greater toxicity to cancer cell line than other cell types, it would be more comprehensive if the authors provide a possible explanation for this selectivity of AIE-COFs to cancer cells.
3. In the revised manuscript, the authors showed that the AIE-COFs mainly located in lysosomes and endoplasmic reticulum, is such distribution of AIE-COFs in MC38 cells can be observed in immune cells? Additionally, is such distribution further contributed to the excellent PDT and PTT effects on cancer cell lines. More importantly, it would be more complete if

the authors provide detailed information on the interanimation pathways of AIE-COFs.
4. In the revised manuscript, the authors showed the maturation of DCs after treatment with AIE-COFs, in order to show the maturation of DCs more specifically, the authors need to locate DCs by staining the markers of DCs such as CD11C, MHCII. Additionally, it would be more complete if the authors conduct a statistical analysis to the immunostaining images.

Version 2:

Reviewer comments:

Reviewer #1

(Remarks to the Author)
Thank you for your thorough revisions and for addressing my previous comments. I appreciate the effort made to clarify the manuscript and ensure the statistical data presentation is transparent and consistent. The manuscript is significantly improved, and I believe it is now in a much stronger position for publication. I have no further concerns at this time.

Reviewer #2

(Remarks to the Author)
The authors have adequately addressed my comments and this is now suitable for publication.

Reviewer #3

(Remarks to the Author)
The re-submitted manuscript entitled “Trigger inducible tertiary lymphoid structure formation using covalent organic frameworks for cancer immunotherapy” have addressed the comments from me and other reviewers comprehensively. The details as well as the organization of data are well improved. However, I still have a few additional concerns as below:

1. The captions of supplementary data are need to be clarified with more detail, such as supplementary figure. 7,30,31.
2. The details on the statistical analysis of figures and supplementary figures in the captions are further needed to be checked throughout the whole manuscript, such as figure 6f, figure 7c, supplementary figure. 15,16,21 as well as 22.

Point-by-Point Response to Reviewers' Comments

Reviewers Comments:

==========

Reviewer #1:

Comments:

The authors propose an innovative approach to induce TLS in vivo for the purpose of treating established cancers in murine preclinical models of cancers. They leverage a novel covalent organic framework methodology and describe a mechanism of antitumor immunity at the single cell level. This work is highly interesting and they should be commended on their efforts.

Response:

We are very grateful to the reviewer for pointing out the novelty of our work. We also highly appreciate the reviewer's careful reading and constructive suggestions that helped us to further the quality. By responding to the reviewer's comments in detail and revising the manuscript accordingly, we believe our manuscript has been significantly strengthened. All revisions are highlighted in BLUE color in the revised manuscript and Supplementary Information.

Comment 1:

1. *"Figure 1 is beautifully constructed but the legend incompletely explains elements in the figure (such as the CellphoneDB algorithm or the role of CTLA-4 inhibition or the primary and distant, presumably synchronous cancers)."*

Response 1:

We thank the reviewer for the valuable suggestion. As recommended, we have added more detailed descriptions to the caption of Figure 1 and highlighted these changes in BLUE in the revised manuscript with details as following:

Fig. 1 Illustration of the design of scRNA-seq aided immunotherapy facilitated by AIE COF-induced TLS formation. The application of AIE COF-mediated phototherapy leads to the induction of TLS formation by stimulating the excessive secretion of key cytokines. This process subsequently promotes the maturation, proliferation, and migration of T and B cells. To explore the underlying mechanisms, single-cell sequencing was utilized, and receptor-ligand interactions between cells were analyzed using CellphoneDB, a tool for characterizing cell-cell communication networks from scRNA-seq data. Notably, the analysis indicated that PD1 expression in T cells did not obviously increase following AIE COF treatment. In contrast, there of CD86 expression, a ligand for CTLA4, was markedly upregulated. Consequently, combining CTLA4 blockade with AIE COF treatment exhibits a higher potential to effectively suppress the growth of both primary and distant tumors.

Comment 2:

2. *"There are too many abbreviations - 18 in the first 2 pages alone! Needs to be addressed."*

Response 2:

We thank the reviewer for their careful observations. As suggested, we have added the full names for the abbreviations and highlighted these changes in BLUE in the revised manuscript.

Comment 3:

3. *"Fig 5 - on what day is the endpoint flow analysis conducted? It would be surprising to see Tcm early in the course of therapy. Would omit T cell changes in spleen - not clear how this relates to antitumor immunity in the TIME or tdLN."*

Response 3:

We sincerely thank the reviewer for their careful observations and apologize for the oversight regarding the timing of flow cytometry detection. In this study, flow cytometry analysis was not carried out during the early stages of treatment. Instead, it was performed 15 days after the initiation of AIE COF treatment, at which point the average tumor volume in the control group had already reached 1000 mm^3. Therefore, our flow analysis was conducted during the mid-to-late stages of the treatment.

Here we included the analysis of T cell changes in the spleen to provide a comprehensive view of the systemic immune response. The results indicated that the spleen is an important site for the generation of memory T cells, which have the ability to respond quickly and provide long-term protection, participate in systemic immune surveillance, and can provide effective immune defense (*Sci. Immunol.* **6**, eabg6895 (2021), *Nat. Commun.* **14**, 5355 (2023)). In addition, T cells in the spleen can migrate to tumor sites to achieve antitumor immunity (*Science* **380**, 203-210 (2023)). At the same time, following the reviewer's suggestion, we have added the data on changes in T cells within the tumor to replace the data on changes in splenic T cells. We found that T cells proportion was increased after TPDA-ViBT-COF+laser treatment, which indicated that TPDA-ViBT-COF+laser treatment is capable of promoting T cell clone retirement.

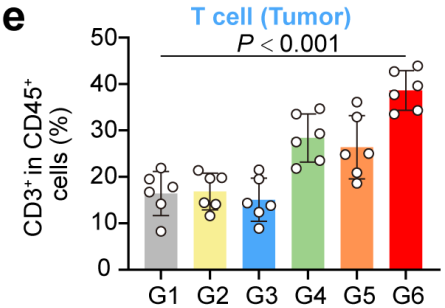

Fig. R1. Quantification of T cell ($CD3^+$) gating on $CD45^+$ cells in tumor, n = 6 independent samples. G1: Control; G2: Laser; G3: TPDA-TPDA-COF; G4: TPDA-TPDA-COF+660 nm; G5: TPDA-BT-COF+660 nm; G6: TPDA-ViBT-COF+660 nm.

Revision made:

In the revised manuscript, we have clearly stated the time point of flow cytometry detection in the results section with details as following:

To delve deeper into the influence of TPDA-ViBT-COF on the immune response of the host organism, we analyzed the changes in immune cells in tumor, tumor draining lymph nodes (TDLN) and spleen (SP) on the 15 days after treatment (Supplementary Fig. 17 to 19).

We have added the data of Fig. R1 as "Fig. 5e" in the revised manuscript.

Comment 4:

4. "*Fig 5 F - are the authors claiming that 60-70% of all CD45 cells in the tdLN are CD3 lymphocytes? This is inconsistent with published data for these well characterized preclinical models (and far outside of what is reasonably expected in a reactive tdLN during IO therapy)*"

Response 4:

We sincerely thank the reviewer for their careful review. Based on your suggestion, we re-examined the original data and conducted a new gating analysis of the flow cytometry data using strict negative controls as a reference (as shown in the Figure R2 below). In the revised manuscript, we have re-evaluated the changes in T cells within the lymph nodes, and based on recalculations, approximately 45-60% of all $CD45^+$ cells in the lymph nodes are T lymphocytes.

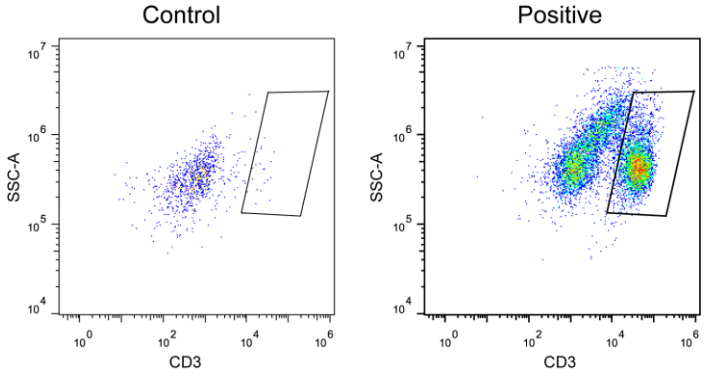

Fig. R2. Gating strategy of the changes in T cells within the lymph nodes.

Revision made:

We have re-evaluated the proportion of CD3 lymphocytes of all CD45 cells in the TDLN with details as following:

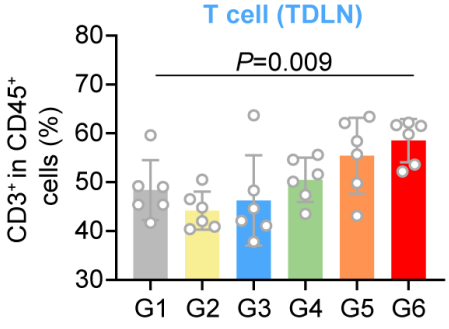

Fig. R3. Quantification of T cell ($CD3^+$) gating on $CD45^+$ cells in tumor, n = 6 independent samples. G1: Control; G2: Laser; G3: TPDA-TPDA-COF; G4: TPDA-TPDA-COF+660 nm; G5: TPDA-BT-COF+660 nm; G6: TPDA-ViBT-COF+660 nm.

The revised gating strategy of T cell was shown in Supplementary Fig. 19. with details as following:

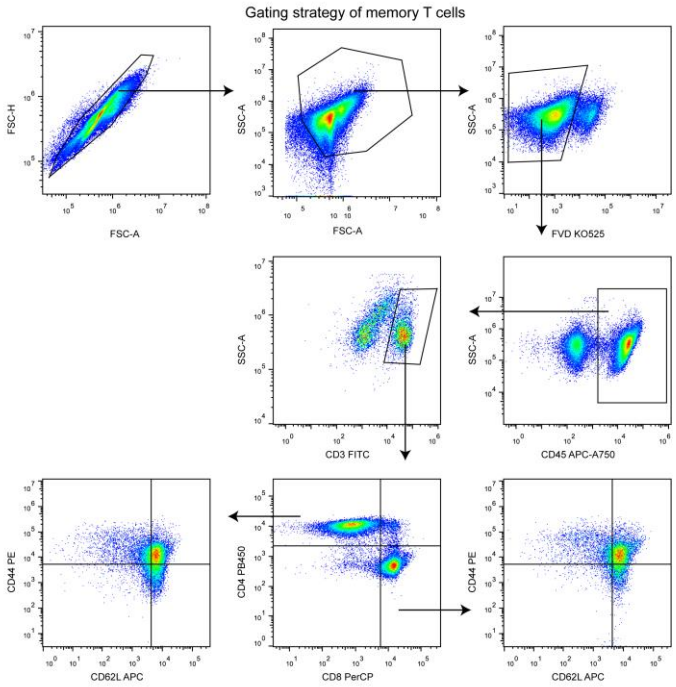

Fig. R4. Gating strategy of dendritic cells (DC) in draining lymph nodes (TDLN).

Comment 5:

5. "*Fig 5 - necessary to explain how the DLN was defined*"

Response 5:

We sincerely thank the reviewer for their careful reading. We would like to clarify that the "DLN" mentioned in the manuscript refers to "TDLN." Accordingly, we have revised the manuscript and highlight in BLUE in the revised manuscript on page 11 line 18. Since the tumor is established near the hind limb on the back of the mouse, the TDLN in this context refer to the inguinal lymph nodes of the mouse.

Revision made:

Accordingly, we have revised the manuscript and highlight in BLUE in the revised manuscript on page 11 line 18, with details as following:

To delve deeper into the influence of TPDA-ViBT-COF on the immune response of the host organism, we analyzed the changes in immune cells in both the tumor draining lymph nodes (TDLN) and spleen (SP) on the 15 day after treatment (Supplementary Fig. 17-19).

Comment 6:

6. "*Fig 6 - Would the authors expect that DCs be present in their TLS? were DCs below the 5% abundance threshold. If indeed below the 5% threshold, authors should strongly consider liberating this threshold to capture these critical immune effectors - particularly in light of the subsequent analysis exploring them by flow and the ELISA work showing significant elevations in CCL19 and CCL21. Please explain*"

Response 6:

We sincerely thank the reviewer for their careful reading. Indeed, dendritic cells play a crucial role in the maturation of TLS. Unfortunately, we still didn't capture DCs even without setting a threshold. This may be due to the limited number of immune cells captured in our scRNA-seq. When the number of cells captured by scRNA-seq is limited, it can affect the capture and accurate identification of some low-abundance cell types such as DCs (*Cell Syst.* **2**, 239-250(2016)). Inspired by the reviewer's insightful comment, we will increase the number of sequencing samples and use techniques such as flow sorting in future studies to enhance the ability of single-cell sequencing to capture specific cell types, allowing for better differentiation and identification of these low-abundance cell types. Additionally, based on the reviewer's suggestion, we recognized the importance of DCs in iTLS. Therefore, we validated the presence of DCs in iTLS using mIHC. We found that after AIE COF treatment, the content of DCs within the tumor was increased, and the DCs can also be clearly observed in the iTLS.

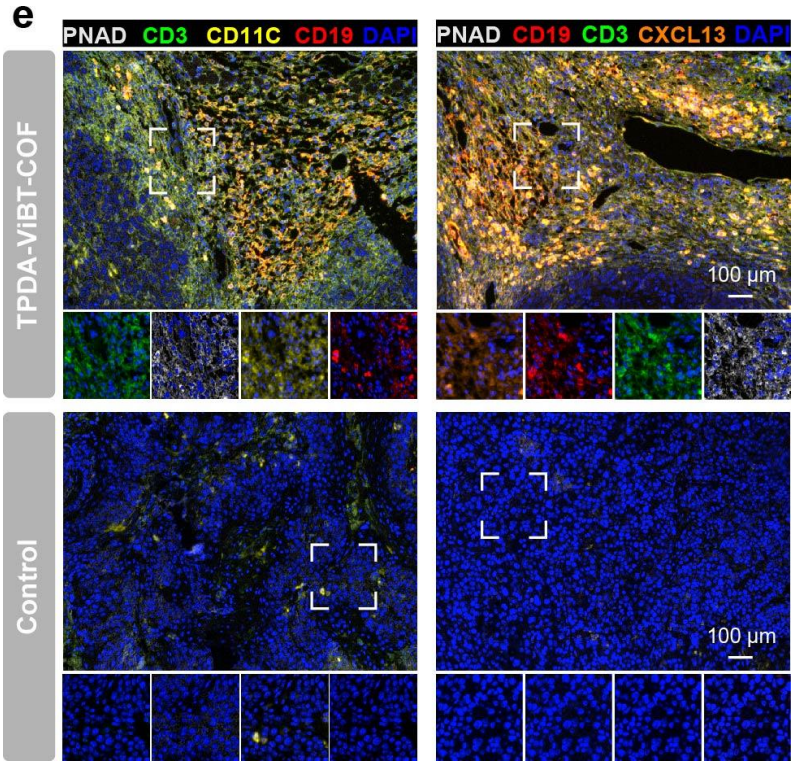

Fig. R5. Representative images of mIHC staining of CD19 (red), CD3 (green), PNAD (grey), CD11C (cyan), CXCL13 (orange), and DAPI (blue) in 4MOSC1 tumor with or without TPDA-ViBT-COF treatment, scale bar = 100 μm.

Revision made:

We have added the data of Fig. R5 as "Fig. 7**e**" in the revised manuscript.

Comment 7:

7. "*Fig 6 E - add statistics*"

Response 7:

We sincerely thank the reviewer for their careful observation. As suggested, we have provided a clear description of the numerical changes in the proportions of different cell types in Fig. 6E.

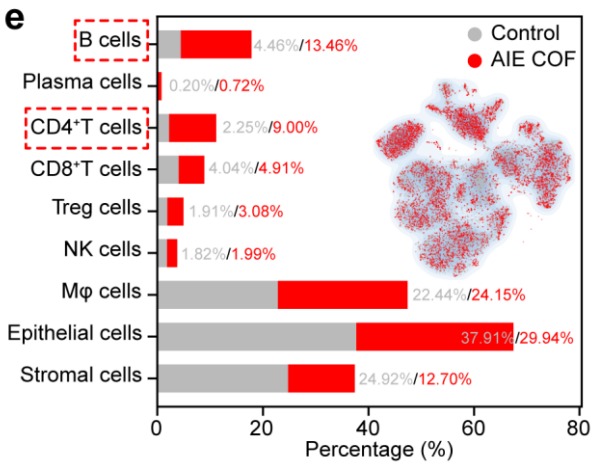

Fig. R6. A stacked histogram was employed to depict the percentages of different cell types among total cells, with or without TPDA-ViBT-COF treatment.

Revision made:

We have added the data of Fig. R6 as "Fig. 6e" in the revised manuscript.

Comment 8:

8. "*Fig 7 - where was 4MOSC1 injected for these experiments? Fig 7 b-d - excellent and convincing (Assuming that the modeling was orthotropic.)*"

Response 8:

We sincerely thank the reviewer for their careful reading. We apologize for omitting the method for establishing the 4MOSC1 tumor-bearing mouse model. In this study, we established the tumor-bearing mouse model by subcutaneously injecting 4MOSC1 tumor cells into the right flank of the mice. To ensure the successful establishment of subcutaneous tumors, a total of 2×10^6 4MOSC1 cells inoculated subcutaneously into the right back of C57BL/6 mice. Detailed methods for constructing the 4MOSC1 tumor model have been

included in the revised Supplementary Materials, with details as following:

In vivo antitumor effects in 4MOSC1-tumor-bearing mice: To established 4MOSC1-tumor-bearing mice animal model, a total of 2×10^6 4MOSC1 cells inoculated subcutaneously into the right back of C57BL/6 mice. The antitumor efficacy of AIE COFs was evaluated using the 4MOSC1-tumor-bearing mouse animal model. Following an eight-day post-injection period, the mice were randomly distributed among six groups with varying treatments (Control, 660 nm laser (1.0 W cm^{-2}, 5 min), TPDA-TDTA-COF, TPDA-TDTA-COF+660 nm (1.0 W cm^{-2}, 5 min), TPDA-BT-COF+660 nm (1.0 W cm^{-2}, 5 min), and TPDA-ViBT-COF+660 nm laser (1.0 W cm^{-2}, 5 min). AIE COFs in a dose of 5 mg kg^{-1} was administered to each group (intratumoral injection), and body weights and tumor volumes were monitored every three days.

Comment 9:

9. "*Fig 8 - what was the tumor model here? add to fig legend and provide relevant methodology for tumor modeling and day of harvest (brief description would assist the reader here)*"

Response 9:

We sincerely thank the reviewer for the valuable suggestion. The tumor model in figure 8 is a MC38-tumor bearing mice, we add it in the figure legend. Additionally, we apologize for omitting the experimental methods related to scRNA-seq of MC38 tumor tissue. We added the specific methods for scRNA-seq of MC38 tumor tissue and the time of tumor harvest and highlight in BLUE in the revised Supplementary Materials with details as following:

Fig. 8. scRNA-seq was used to dissect the potential immunotherapy targets for TPDA-ViBT-COF-mediated phototherapy in MC38-tumor bearing mice.

ScRNA-seq: 1×10^6 MC38 cells were inoculated in the right blank C57BL/6 mouse to establish MC38-tumor-bearing mice. Following an eight-day post-injection period, the mice were randomly distributed among two groups with varying treatments (Control, 660 nm laser (1.0 W cm^{-2}, 5 min) and TPDA-ViBT-COF+660 nm laser (1.0 W cm^{-2}, 5 min). On day 15 post-phototherapy, the C57BL/6 mice were euthanized, and the tumors were harvested. The tumors were then processed into single-cell suspensions, with a cell concentration of 700-1200 cells μL^{-1} for each sample for ScRNA-seq. The MobiCube Single-Cell 3' RNA-seq Kit v1.0 (MobiDrop) was used to prepare the library, which was subsequently sequenced using Illumina NovaSeq 6000 Systems. Normalized aggregate data was generated across the samples using the MobiVision software pipeline (version 1.1, MobiDrop). This process involved demultiplexing cellular barcodes, mapping reads to the genome and transcriptome using STAR solo, and down-sampling reads as needed. The resulting output data yielded a matrix of gene counts versus cells.

Comment 10:

10. "*Gating strategies in supp need have the decades added to the axes*"

Response 10:

We sincerely thank the reviewer for such careful observation. As the reviewer suggested, we added decades to the axes of the Gating strategies in the Supplementary Materials and highlight in BLUE, with details as following:

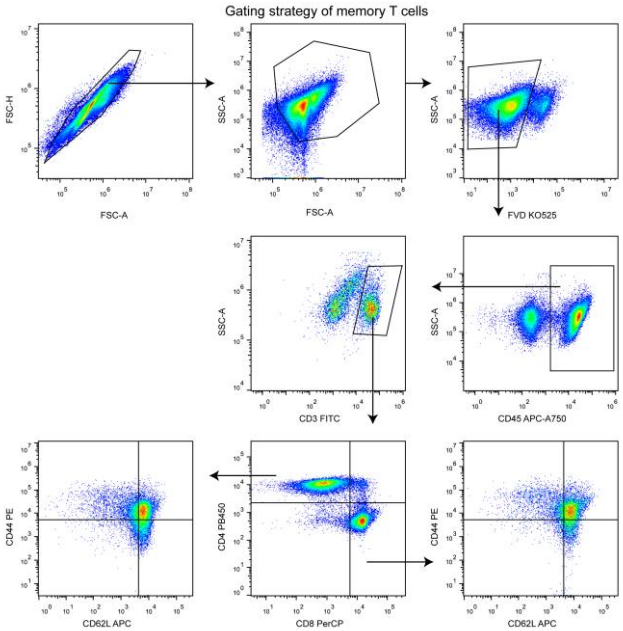

Fig. R7. Gating strategy of memory T cells.

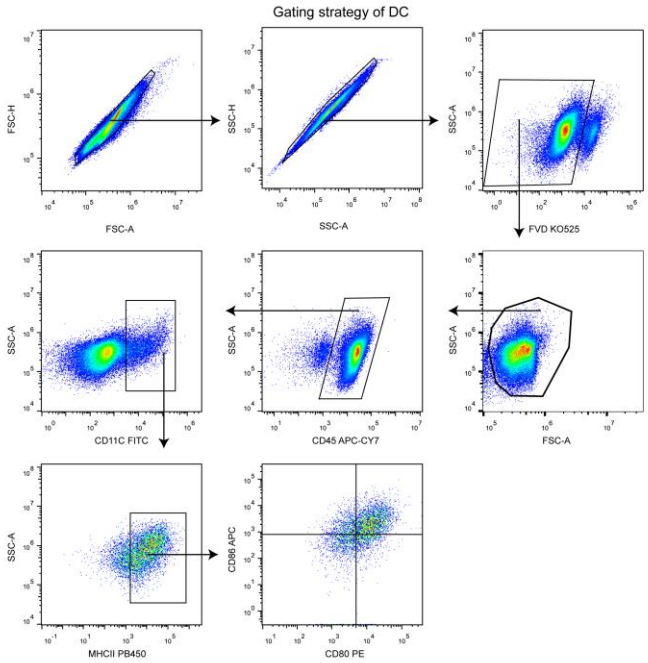

Fig. R8. Gating strategy of dendritic cells (DC) in draining lymph nodes (TDLN).

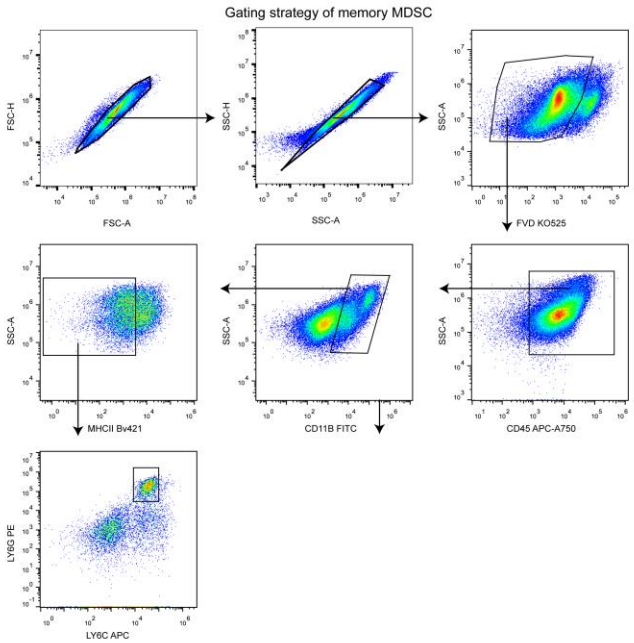

Fig. R9. Gating strategy of myeloid-derived suppressor cells (MDSCs) in spleen.

Comment 11:

11. "*Supp Fig 15 - the gate for CD44 v CD62L looks to be inappropriately placed. The true CD44$^+$ population looks to be at a higher decade than where the authors have placed the gate (as it is now, it looks to be bisecting the CD44- population)*"

Response 11:

We sincerely thank the reviewer for such careful reading. As the reviewer suggested, we have revised our gating strategy and re-evaluated the CD4$^+$ and CD8$^+$ central memory T cells, and highlight in BLUE in the revised Supplementary materials, with details as following:

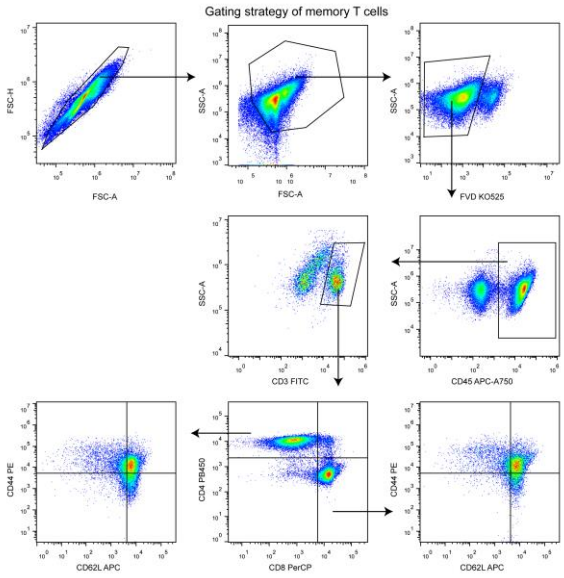

Fig. R10. Gating strategy of dendritic cells (DC) in tumor draining lymph nodes (TDLN).

At the same time, we also re-evaluated the proportion changes of $CD4^+$ and $CD8^+$ central memory T cells in both TDLN and spleen in the revised manuscript, with details as follows:

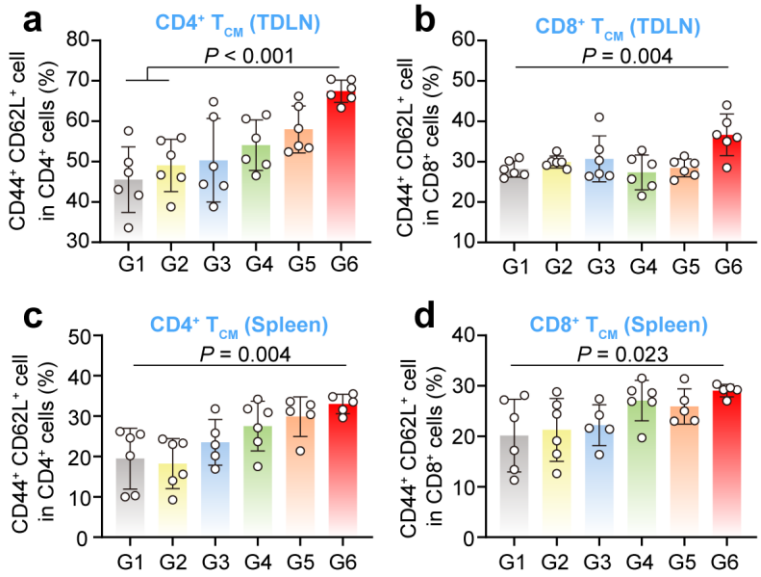

Fig. R11. (**a** to **d**) Quantification the gating of $CD4^+$ T_{CM}/$CD8^+$ T_{CM} ($CD44^+CD62L^+$) on $CD3^+$ $CD4^+$/ $CD8^+$ in both DLN and spleen, n = 6 independent samples. G1: Control; G2: Laser; G3: TPDA-TPDA-COF; G4: TPDA-TPDA-COF+660 nm; G5: TPDA-BT-COF+660 nm; G6: TPDA-ViBT-COF+660 nm.

Comment 12:

12. "*Fig 5 & Supp Fig 17 - would not expect MDSCs in the spleen in a preclinical tumor model. this should be addressed and explored in the TIME*"

Response 12:

We sincerely thank the reviewer for such careful reading. As suggested, we investigated the changes in the proportion of myeloid-derived suppressor cells (MDSCs) within the tumor. The results indicate that the proportion of MDSCs is markedly decreased following treatment with TPDA-ViBT-COF+laser.

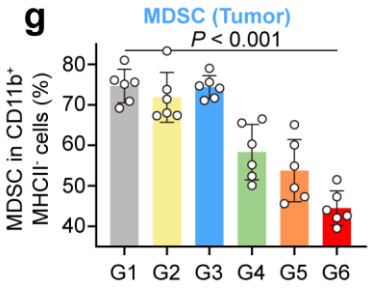

Fig. R12. Quantification of MDSC ($Ly6G^{high}$ $Ly6C^{low}$) gating on $CD11b^+$ $MHCII^-$ cells in the tumor, n = 6 independent samples. G1: Control; G2: Laser; G3: TPDA-TPDA-COF; G4: TPDA-TPDA-COF+660 nm; G5: TPDA-BT-COF+660 nm; G6: TPDA-ViBT-COF+660 nm.

Revision made:

We have added the data of Fig. R12 as "Fig. 5**g**" in the revised manuscript.

Comment 13:

13. "*Supp 25 - need to add CXCL13 label to the figure*"

Response 13:

We sincerely thank the reviewer for such careful reading. As the reviewer suggested, we added the CXCL13 label to Supplementary Fig. S27, with details as following:

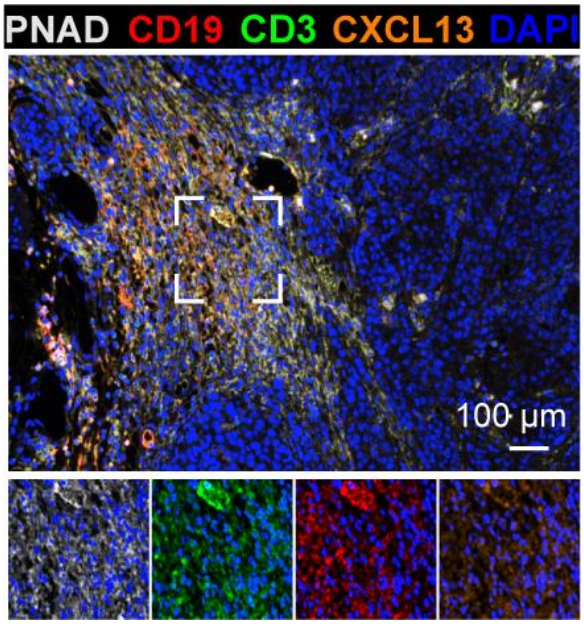

Supplementary Fig. 27. Representative images of mIHC staining of CD19 (red), CD3 (green), PNAD (grey), CXCL13 (orange), and DAPI (blue) in 4MOSC1 tumor with or without TPDA-ViBT-COF treatment, scale bar = 100 μm.

Comment 14:

14. "*Methods for in vitro/in vivo 4MOSC is needed*"

Response 14:

We sincerely thank the reviewer for such careful reading. We apologize for forgetting offer the detailed methods for the *in vitro* culture and *in vivo* experiments of 4MOSC1. As suggested, we have added these details methods in the revised manuscript and the Supplementary Materials, with details as following:

The murine squamous carcinoma cell line 4MOSC1 is gifted from Prof. J. Silvio Gutkind of the University of California San Diego *via* a material transfer agreement (SD2017-202). The 4MOSC1 cells were cultured in Keratinocyte serum-free medium (K-SFM, Gibco) culture conditions at 5% CO_2 and 37 °C.

In vivo antitumor effects in 4MOSC1-tumor-bearing mice: To established 4MOSC1-tumor-bearing mice animal model, a total of 2×10^6 4MOSC1 cells inoculated subcutaneously into the right back of C57BL/6 mice. The antitumor efficacy of AIE COFs

was evaluated using the 4MOSC1-tumor-bearing mouse animal model. Following an eight-day post-injection period, the mice were randomly distributed among six groups with varying treatments (Control, 660 nm laser (1.0 W cm^{-2}, 5 min), TPDA-TDTA-COF, TPDA-TDTA-COF+660 nm (1.0 W cm^{-2}, 5 min), TPDA-BT-COF+660 nm (1.0 W cm^{-2}, 5 min), and TPDA-ViBT-COF+660 nm laser (1.0 W cm^{-2}, 5 min). AIE COFs in a dose of 5 mg kg^{-1} was administered to each group (intratumoral injection), and body weights and tumor volumes were monitored every three days.

Comment 15:

15. "*Can the authors please comment and add a non-tumor model in vivo to convincingly demonstate that their TPDA-ViBT-COF+Laser does indeed lead to the minimal components and 3-D anatomy of recognized TLS. As is, only representative IF images are proposed for the readers to support TLS formation. Given that this work leverages a novel approach to induce TLS it is critical that an independent, validated and well-used model is needed to convincingly demonstrate iTLS.*"

Response 15:

We sincerely thank the reviewer for such insightful comment. As suggested, we constructed a non-tumor model by injecting TPDA-ViBT-COF subcutaneously into mice upon laser irradiation. Through mIHC, we found that the content of T cells and B cells increased in the skin tissue treated with TPDA-ViBT-COF. These structures are important components of TLS, but the distribution of T cells and B cells was too loose and insufficient to trigger the formation of TLS. This result indicates that it's hard to induce the formation of TLS in non-tumor tissue although TPDA-ViBT-COF mediated phototherapy. The reason for this phenomenon may be that the formation of iTLS induced by TPDA-ViBT-COF relies on its cytotoxic effect on tumor cells and the subsequent release of tumor antigens and inflammatory cytokines (*J. Dent. Res.* **102**, 678-688 (2023)). In the non-tumor model, the absence of tumor cells may limit the ability of TPDA-ViBT-COF to recruit immune cells, as well as the role of tumor antigens released by dead tumor cells in the activation and proliferation of immune cells (*Nat Rev Cancer* **19**, 307-325(2019); *Nat Rev Cancer* **22**, 414-430 (2022)). Additionally, to more clearly characterize the iTLS structure, we further labeled important structures such as high endothelial venules and dendritic cells using mIHC in our revised manuscript. We hope that these supplementary experiments will make our iTLS more convincing.

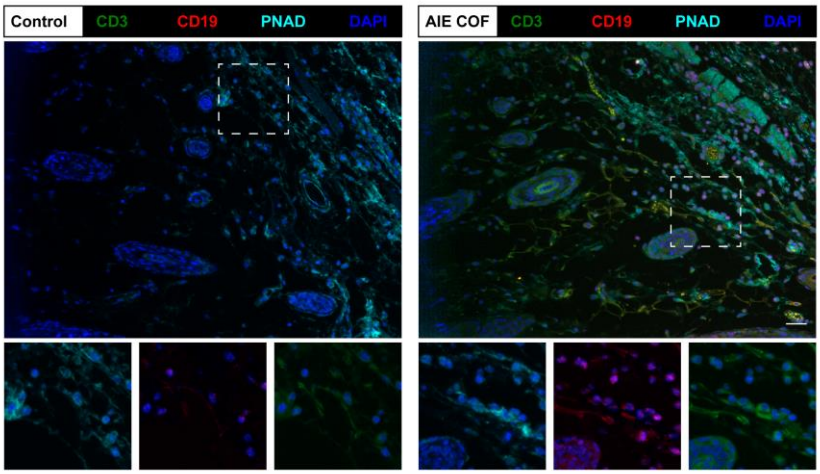

Fig. R13. Representative images of mIHC staining of CD19 (red), CD3 (green), PNAD (white), and DAPI (blue) in non-tumor tissue with or without TPDA-ViBT-COF treatment, scale bar = 100 μm.

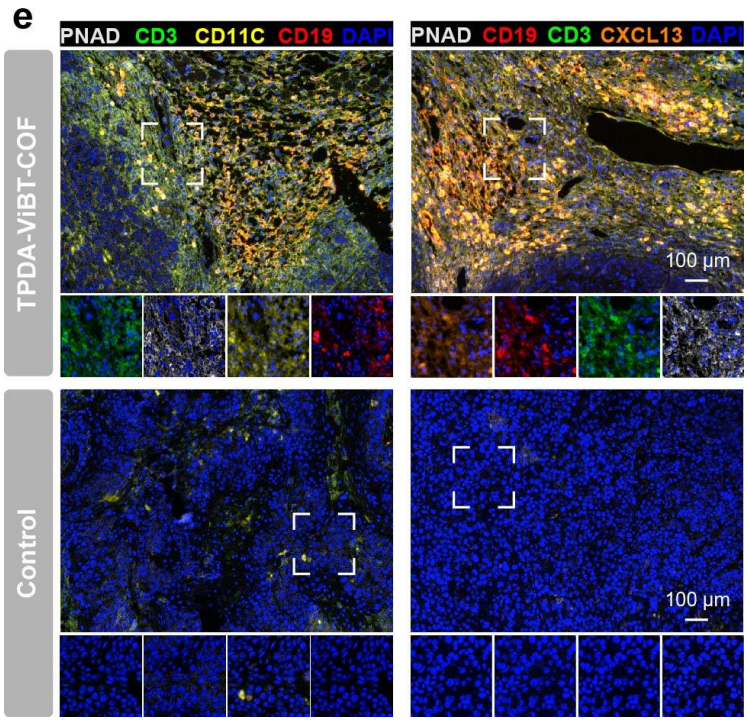

Fig. R14. Representative images of mIHC staining of CD19 (red), CD3 (green), PNAD (white), CD11C (yellow), CXCL13 (orange), and DAPI (blue) in 4MOSC1 tumor with or without TPDA-ViBT-COF treatment, scale ba r= 100 μm.

Comment 16:

16. "*Can the authors please provide data indicating the number of iTLS within tumors and the % volume of iTLS relative to total tumor volume. Do these analyses fit with what has been reported in the literature?"*

Response 16:

We sincerely thank the reviewer for their valuable suggestion. Based on your suggestion, we provided data indicating the number of iTLS within tumors. We are apologized that TLS volume cannot be accurately calculated due to the irregular shape of TLS three-dimensional structure. But we have utilized immunohistochemistry to calculate the area of B cell aggregation in the tumor tissue and preliminarily estimated the area percentage of AIE COF-induced iTLS based on tumor tissue sections. We found that in the AIE COF treated MC38 tumor tissues, the number of TLS was approximately 1-2, accounting for an average of 1.40% of the total tumor tissue section area. In the 4MOSC1 tumor tissues, the number of TLS was approximately 1-3, accounting for 3.17% of the total tumor tissue section area.

Due to current research on TLS primarily focuses on the presence or absence of TLS and its impact on ICB therapy, with relatively few studies on the quantification of TLS in different tumors. Moreover, iTLS induced by AIE COF may be difficult to compare with naturally occurring TLS in human tumors or TLS in mouse tumor models induced by different methods.

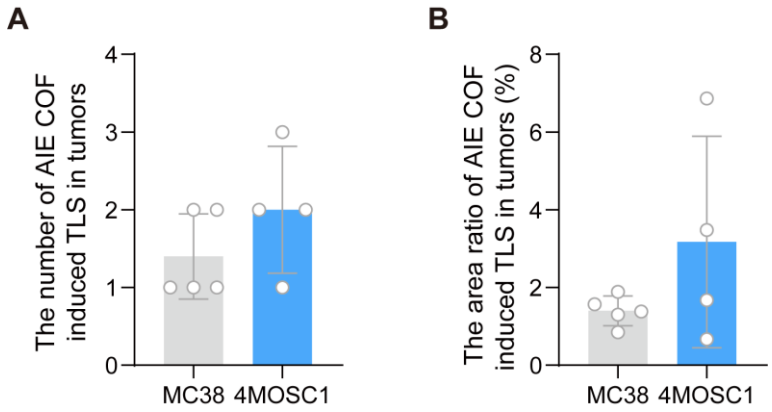

Fig. R15. (A) The number of AIE COF induced TLS in MC38 and 4MOSC1 tumor. (B) The area ratio of AIE COF induced TLS in MC38 and 4MOSC1 tumor.

Revision made:

We have added the data of Fig. R15 as "Supplementary Fig. 30" in the Supplementary Information and highlighted in BLUE on page 36.

Comment 17:

17. "*The discussion is incomplete - need to add context for iTLS methodology and context for how the immuno-mechanistic findings with their iTLS fit into the existing literature. For example, the T cell infiltration data and ELISA with CCL19/CCL21 would suggest a critical role for DCs (as might be expected) but this is underexplored.*"

Response 17:

We sincerely thank the reviewer for their insightful comments. As the reviewer suggested, we add more discussions about the ELISA with CCL19/CCL21 in revised the manuscript and

highlight in BLUE in the revised manuscript, with details as following:

Previous studies have demonstrated that tumor cells release inflammatory cytokines such as TNFα, IFNγ, and CXCL10 under stress conditions.[69-71] In this study, we found that the AIE COF-mediated phototherapy effectively promotes the release of these inflammatory factors by inducing thermal and chemical damage directly to the tumor cells. These dying tumor cells can then act as an in situ vaccine, activating DCs. Subsequently, mature DCs secrete cytokines such as CCL19 and CCL21, to facilitate the recruitment of T cells and B cells into the tumor, allowing the formation of T cell zones and B cell zones within the TLS.[72-73] Furthermore, the inflammatory cytokines secreted by tumor cells, including CXCL10, TNFα, IFNγ, and IFNβ, promote the localization and maturation of T lymphocytes within the TME.[69] We also confirmed increased intratumoral T cell infiltration using scRNA-seq and flow cytometry analysis. Our scRNA-seq data validated that this increase in T cell content was accompanied by elevated levels of T cell-associated cytokines, such as IL22, IL7, and IL13, which are essential for B cell maturation and proliferation.[74-76] In addition, the mIHC results also unveiled that mature dendritic cells and dying tumor cells, along with inflammatory cytokines, facilitate the recruitment and proliferation of B cells and T cells, ultimately forming B cell and T cell clusters within the TLS.

Comment 18:

18. "*references 5, 6, 12, 24 are not appropriately assigned to the corresponding claims in the text*"

Response 18:

We sincerely thank the reviewer for such careful reading. As the reviewer suggested, we add some new references and highlight in BLUE in the revised manuscript, with details as following:

5. Sacco, A. G. et al. Pembrolizumab plus cetuximab in patients with recurrent or metastatic head and neck squamous cell carcinoma: an open-label, multi-arm, non-randomised, multicentre, phase 2 trial. *Lancet Oncol.* **22**, 883-892 (2021).

6. Seiwert, T. Y. et al. Safety and clinical activity of pembrolizumab for treatment of recurrent or metastatic squamous cell carcinoma of the head and neck (KEYNOTE-012): an open-label, multicentre, phase 1b trial. *Lancet Oncol.* **17**, 956-965 (2016).

12. Derks, S. et al. Characterizing diversity in the tumor-immune microenvironment of distinct subclasses of gastroesophageal adenocarcinomas. *Ann. Oncol.* **31**, 1011-1020 (2020).

24. Helmink B. A. et al. B cells and tertiary lymphoid structures promote immunotherapy response. *Nature*, **577**, 549-555 (2020).

Comment 19:

19. "*references Wang-Gutkind Nat Comm 2021 and Saddawi-Gutkind Nat Comm 2022 should be added to ref 64*"

Response 19:

As the reviewer suggested, we add these references to ref 64 and highlight in BLUE in the revised manuscript, with details as following:

65. Wang Z. *et al*. Disruption of the HER3-PI3K-mTOR oncogenic signaling axis and PD-1 blockade as a multimodal precision immunotherapy in head and neck cancer. *Nat Commun*, **12**, 2383 (2021).

66. Saddawi-Konefka R. *et al*. Lymphatic-preserving treatment sequencing with immune checkpoint inhibition unleashes cDC1-dependent antitumor immunity in HNSCC. *Nat Commun*, **13**, 4298 (2022).

Comment 20:

20. "*Please elaborate on how COFs and the formation of pearls relate. This is unclear and should be explained in the introduction with the appropriate reference. Additionally, if space allows, it should be explained concisely (briefly) in the abstract. It is clearly a feature of novelty that the authors have capitalized upon, but it is also very unfamiliar to the readers who will likely be attracted to this paper for its relation to antitumor immunity and IO and TLS.*"

Response 20:

We sincerely thank the reviewer for their constructive suggestion. As the reviewer suggested, we explain the coordination of COFs and the formation of pearls, and highlight in BLUE in the revised manuscript, with details as following:

The formation of TLS usually necessitates a sustained inflammatory environment, akin to the prolonged period required for the formation of pearls following the implantation of a bead nucleus in artificial cultivation. Inspired by the mechanism of pearl cultivation, we hypothesize that COF-based nanomedicine may function similarly to the bead nucleus, owing to their outstanding performance in eliciting chronic inflammatory microenvironment which may ensure the successful formation of TLS and consequently promote the response rate of cancer immunotherapy.

Comment 21:

21. "*This sentence follows a claim regarding the limitation of TLS in cancer (below). It's an awkward transition and unclear how the concepts are connected. Re-writing is recommended. Notably, the application of nanomedicines in cancer therapy has garnered significant attention owing to their excellent modifiability, targeting capability, functionality, and immune evasion properties.*[17-23] *What's a MOF? not defined in introduction*"

Response 21:

We sincerely thank the reviewer for such careful reading. As the reviewer suggested, we

rewrite this sentence and highlight in BLUE in the revised manuscript with details as following:

Despite extensive research efforts dedicated to exploring the role of chemokines, cytokines, antibodies, and antigen-presenting cells in driving the formation of tumor-associated lymphoid structures, the number of effective nanomedicine-based TLS formation inducers reported so far remains limited.[9,13-16] Nanomedicines, such as metal-organic frameworks (MOFs) and covalent organic frameworks (COFs), has garnered considerable attention in cancer therapy owing to their excellent modifiability, targeting capability, functionality, and immune evasion properties.[17-23]

Reviewer #2:

Comments:

Zhang et al. present a well written article titled 'Trigger inducible tertiary lymphoid structure formation using covalent organic frameworks for cancer immunotherapy' in which they develop an artificial covalent organic framework for intra-tumor injection to induce tertiary lymphoid structure and anti-tumor immunity. The strength of this article is in optimizing this artificial nanostructure and its photothermal effects in inducing these effects. The article would be strengthened by addressing the following points:

Response:

We are very grateful to the reviewer for their careful reading and pointing out the novelty of our work. We also highly appreciate the reviewer's suggestion for strengthening our work. By responding to the reviewer's comments in detail and revising the manuscript accordingly, we believe that our manuscript has been significantly strengthened. All revisions are highlighted in BLUE color in the revised manuscript and Supplementary Information.

Comment 1:

1. "*Tertiary lymphoid structures should be more clearly defined. In multiple areas in the article, the authors describe them as aggregates of B cells interspersed with T cells. more peripherally CD31 vasculature presence in mentioned. Tertiary lymphoid structures generally require the full architecture of lymph nodes including high endothelial venules so better definition would be appreciated.*"

Response 1:

We thank this reviewer for their insightful comment. As the review suggested, we labeled the high endothelial venules within the tumor using a PNAD antibody and observed PNAD expression in the tertiary lymphoid structure areas.

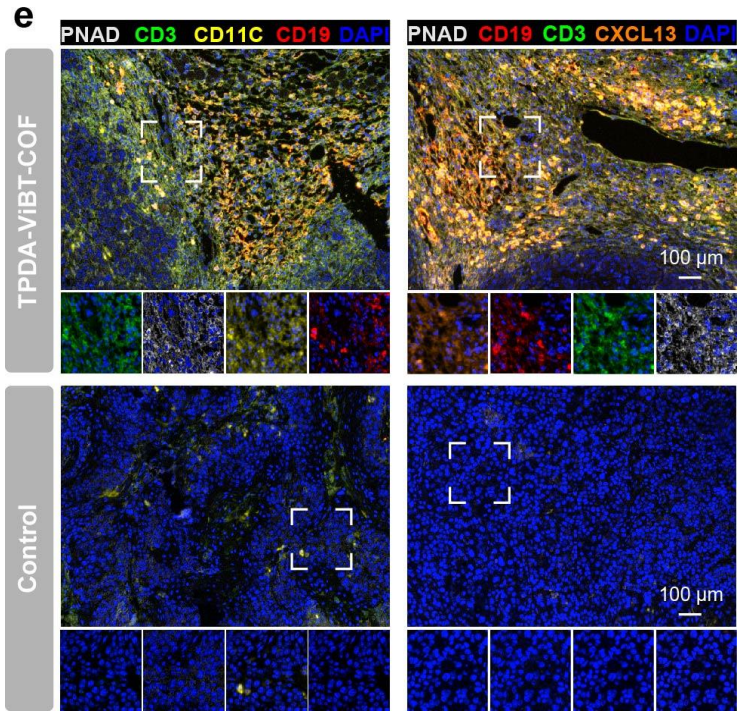

Fig. R16. Representative images of mIHC staining of CD19 (red), CD3 (green), PNAD (white), CD11C (yellow), CXCL13 (orange), and DAPI (blue) in 4MOSC1 tumor with or without TPDA-ViBT-COF treatment, scale bar=100 μm.

Revision made:

We have added the data of Fig. R16 as "Fig. 7e" in the revised manuscript.

Comment 2:

2. "*In terms of models used, the authors selected a model in which other modalities have induced tertiary lymphoid structures. How is their methodology superior to other modalities previously tested that have induced TLS? For their second model they state they selected a model that is notable for its immune cell infiltration which I am presuming means high immune cell infiltration? Can they generate TLS in less immunogenic model as well?*"

Response 2:

We thank the reviewer for the insightful comments. Actually, the application of nanomedicines to facilitate TLS formation remains largely unexplored. Compared to other nanomedicines such as MOFs and metal complexes, COFs are composed solely of light atoms (C, H, O, N), which affords them good degradability and eliminates the potential toxicity associated with metal ions. Additionally, COFs exhibit superior light absorption and photostability compared to small molecules, making them promising candidates for phototherapy applications. Furthermore, the COF-based nanomedicine utilized in this study is capable of eliciting a vigorous and sustained inflammatory response, creating a chronic inflammatory microenvironment that may ensure successful TLS formation.

We chose two tumor models with high immune infiltration to induce TLS formation. Among these models, the 4MOSC1 model exhibits an even higher degree of immune infiltration compared to the MC38 tumor model. Current perspectives suggest that TLS can only be effectively induced in "hot" tumors through persistent antigen and inflammatory stimulation, while "cold" tumors are difficult to induce TLS formation (*Nat. Rev. Cancer.* **19**, 307-325 (2019); *Nat. Rev. Cancer.* **22**, 414-430 (2022)). Our previous research also confirmed that it is hard to induce TLS formation in cold tumors (*J. Dent. Res.* **102**, 678-688 (2023)). As shown in the Fig. R17 below, we examined the cold tumor tissues (4T1) treated with AIE COF. The results indicated an increase in T cells and DC cells in the tumor tissues treated with AIE COF, but no B cells or typical TLS formation were observed, suggesting the it is hard to induce TLS formation in cold tumors.

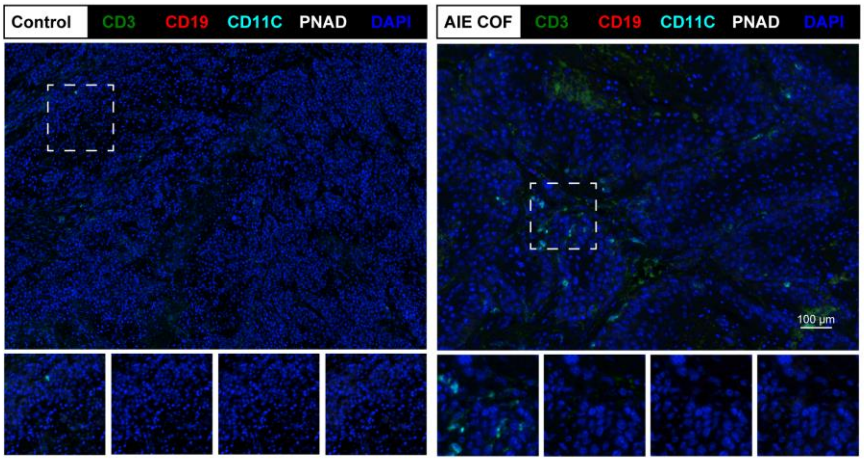

Fig. R17. Representative images of mIHC staining of CD19 (red), CD3 (green), PNAD (white), CD11C (light blue), and DAPI (blue) in 4T1 tumor with or without TPDA-ViBT-COF treatment, scale bar = 100 μm.

Comment 3:

3. "*Figure 1 is dense but it is not clear what exactly it is showing. Better description in caption would be important.*"

Response 3:

Thanks for the reviewer's insightful comment. As the review suggested, we add more descriptions in the caption of figure 1, and highlight in BLUE in the revised manuscript with details as following:

Fig. 1 Illustration of the design of scRNA-seq aided immunotherapy facilitated by AIE COF-induced TLS formation. The application of AIE COF-mediated phototherapy leads to the induction of TLS formation by stimulating the excessive secretion of key cytokines. This process subsequently promotes the maturation, proliferation, and migration of T and B cells. To explore the underlying mechanisms, single-cell sequencing was utilized, and receptor-ligand interactions between cells were analyzed using CellphoneDB, a tool for characterizing cell-cell communication networks from scRNA-seq data. Notably, the analysis indicated that PD1 expression in T cells did not obviously increase following AIE COF treatment. In contrast, there of CD86 expression, a ligand for CTLA4, was markedly upregulated. Consequently, combining CTLA4 blockade with AIE COF treatment exhibits a higher potential to effectively suppress the growth of both primary and distant tumors.

Comment 4:

4. "*Figure 3. Abbreviations should be defined within figure/legend.*"

Response 4:

Thanks for the reviewer's careful reading. As the review suggested, we defined these abbreviations in figure 3 and highlight in BLUE in the figure legend, with details as following:

Fig. 3. Photophysical properties of TPDA-TDTA-COF, TPDA-BT-COF and TPDA-ViBT-COF. (**a**) Illustration of the advantages of TPDA-ViBT-COF. Ultraviolet-visible absorption spectra (**b**), band energy (**c**), solid-state photoluminescence (PL) spectra (**d**), steady-state PL spectra (**e**), quantum yield (**f**) and time-resolved PL spectra (**g**) of AIE COFs. (**h**) Density functional theory calculations of the bandgap of TPDA-TDTA-COF, TPDA-BT-COF and TPDA-ViBT-COF, HOMO: highest occupied molecular orbital; LUMO: lowest unoccupied molecular orbital. Source data are provided as a Source Data file.

Comment 5:

5. "*Figure 5. Bar graphs are hazy and not bright in colors.*"

Response 5:

Thanks for the reviewer's careful observation. As the review suggested, we revised the figure 5 with **black** color, with details as following:

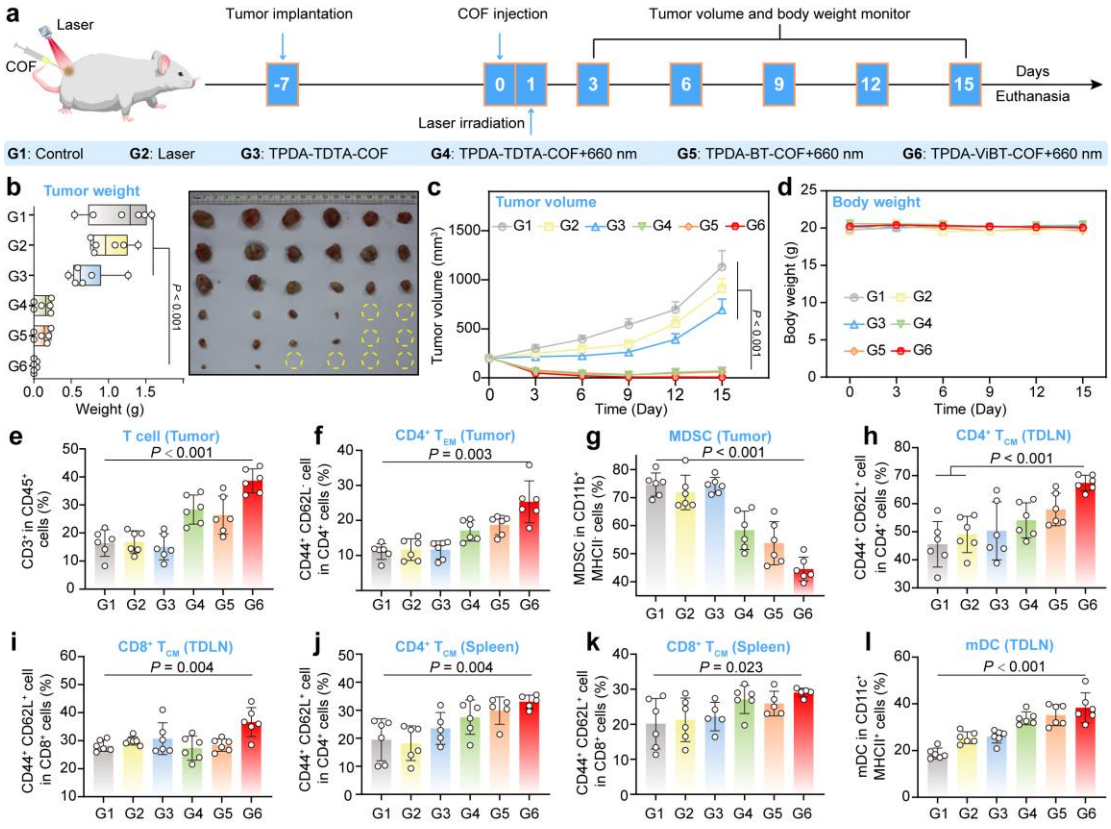

Comment 6:

6. "*Figure 6 shows cytokine secretion at bulk tumor level. Does single cell suggest what cells may be accounting for increased secretion of these?*"

Response 6:

We thank the reviewer for their insightful comment. The results of single-cell RNA sequencing (scRNA-seq) indicated an increase in the proportions of $CD4^+$ T cells and B cells, but still hardly to identify what cells may be accounting for increased secretion of these cytokine. We prioritized the detection of cytokines related to the recruitment of T cells and B cells in downstream experiments, as shown in Figure 6f. We also attempted to detect the

expression of these cytokines through scRNA-seq. Among these cytokines, scRNA-seq only captured *Ifng*, and its detected value was extremely low (Fig. R18), rendering it unsuitable as a reference for subsequent experiments. This phenomenon may due to the limitations of scRNA-seq, where gene-expression profiles are extremely sparse, with 80%-90% of genes undetected in every cell, a phenomenon known as "gene dropout" (*Cell* **184**, 2988-3005 (2021)). This largely limits the ability of scRNA-seq to detect some low-expression molecules, such as transcription factors and cytokines. Moreover, compared to ELISA, transcriptome sequencing methods such as scRNA-seq and bulk RNA-seq are not optimal for quantifying cytokine levels (*Immunity* **53**, 878-894 2020). Therefore, we used ELISA to measure the levels of different cytokines within the tumor.

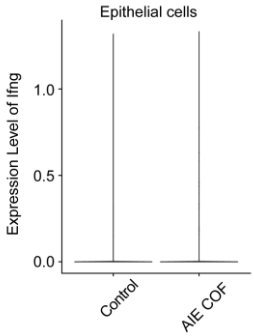

Fig. R18. Violin plot was utilized to depict the expression levels of *Ifng* in Epithelial cells.

Comment 7:

7. "*The authors state COF is associated with reduction in proportion of epithelial and stromal cells and that this suggests elimination of tumor and tumor fibroblast cells. It is instead possible that there is an increase in immune cell proportion due to inflammation but not necessarily elimination of other cell types but just relatively reduction in number as secondary effect.*"

Response 7:

Thanks for the reviewer's careful reading and we apologize for the inaccurate description in our manuscript. The reduction in the proportions of tumor cells and fibroblasts can indeed be influenced by the increase in immune cell proportions. Based on the reviewer's suggestion, we revised this sentence and highlight in BLUE in the revised manuscript (page 13, line 13 to 19) with details as following:

In this work, a sharp reduction in the proportion of epithelial (tumor) and stromal cells and a notable increase in B cells and $CD4^+$ T cells was observed after treatment with TPDA-ViBT-COF (Fig. 6d to e). This may be attributed to the cytotoxic effect of TPDA-ViBT-COF-mediated phototherapy reducing the proportion of tumor cells. Additionally, the release of tumor antigens and inflammatory cytokines increases the infiltration of immune effector cells. The reduction in the tumor and stromal cell ratio, combined with the increase in immune cell proportion, collectively leads to a decrease in the

proportion of non-immune cells.

Comment 8:

8. "*For discussion of scRNAseq, perhaps better phrasing that this suggests CTLA-4 blockade may be better partner than PD-1 blockade would be better rather than saying scRNAseq itself shows that CTLA-4 blockade 'exhibits synergistic effects'. Another part states 'conducted scRNAseq to investigate therapeutic efficacy of …in combination with different checkpoint blockade.' Would soften the language and rephrase.*"

Response 8:

Thanks for the reviewer's valuable suggestion. As the review suggested, we revised this sentence and highlight in BLUE in the revised manuscript (page 17, line 9 to 12) with details as following:

Herein, we try to utilize scRNA-seq to investigate an appropriate immune checkpoint when combined with TPDA-ViBT-COF-mediated phototherapy. The results indicated that CTLA-4 blockade may be a better partner than PD-1 blockade when combined with TPDA-ViBT-COF-mediated phototherapy.

Comment 9:

9. "*In discussion that PD-1 blockade may not be suitable given lower CD8 Tex on scRNAseq, as PD-1 blockade is also relevant in setting of myeloid cell PD-L1 expression, this should also be stated. Additionally, it is possible CTLA-4 displays higher expression in setting of T cell activation. Similarly, the discussion on CD86 having higher expression with treatment is consistent with immune inflammation and activation. Overall the single cell rna sequencing support for why CTLA-4 rather than PD-1 blockade is not as convincing (in vivo data on other hand more supportive) so would perhaps rephrase.*"

Response 9:

Thanks for the reviewer's insightful comments. Indeed, the expression of PDL1 not only on myeloid cells but also on fibroblasts and tumor cells can affect the efficacy of PD1 blockade. Therefore, we examined the overall expression of PDL1 in the tumor tissue using immunofluorescence. The results showed that, in comparison to the control group, there is no apparent increase in PDL1 expression in the AIE COF treated tumor. Similarly, flow cytometry analysis revealed no noticeable increase in PDL1 expression in $CD45^-$ cells.

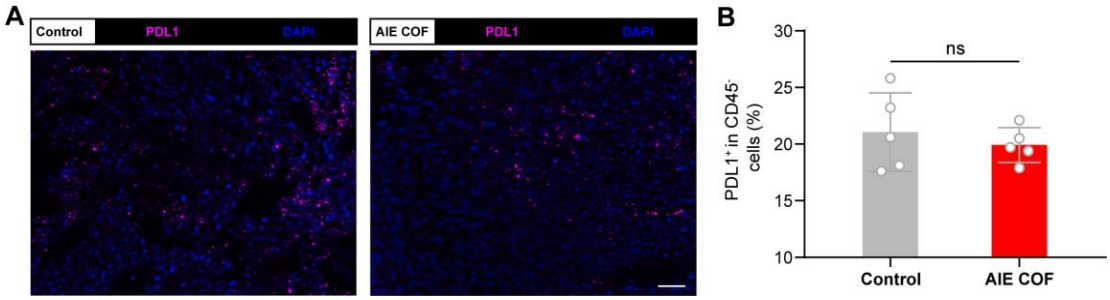

Fig. R19. (a) Immunofluorescence images of PD-$L1^+$ cells before and after treatment in tumor, scale bar = 50 μm. (b) Quantification of PD-$L1^+$ cells gating on $CD45^-$ cells in tumor, n = 5 independent samples.

Revision made:

As the review suggested, we rewrite these sentence and highlight in BLUE in the revised manuscript (page 18) with details as following:

As PD-1 blockade is also relevant in setting of myeloid cell PD-L1 expression, we also assessed PD-L1 expression following TPDA-ViBT-COF combined with laser treatment. The results showed that PD-L1 expression remained very low. Collectively, these results suggest that PD-1 may not be an appropriate target for synergistic therapy in this study (Fig. 8b).

We have also added the data of Fig. R19 as "Supplementary Fig. 31." In the revised Supplementary Information and highlighted in BLUE on page 37.

Comment 10:

10. "*It would be helpful for discussion to include how this would be translated to patients which would presumably be intra-tumoral injection. How would this be activated by laser, etc?*"

Response 10:

Thanks for the reviewer's insightful comment. As the review suggested, we add the discussion of how to translated to patients. and highlight in BLUE in the revised manuscript (page 21) with details as following:

The 660 nm laser used in this study has limited penetration depth. For superficial tumors, intratumoral injection is an effective administration strategy, ensuring that the treatment is localized directly within the tumor, thereby maximizing efficacy while minimizing systemic exposure and potential side effects. For deeper tumors, we propose that intravenous injection of COF nanomedicines with near-infrared-II window absorption, coupled with the subcutaneous implantation of wearable laser devices, could enhance the feasibility of translating this technology into clinical applications.

Comment 11:

11. "*Given the authors are able to induce formation of these structures, it would be helpful to better understand which exact component is contributing to their formation if there is one? Is it a specific cytokine or specific immune cell type? Alternatively, is it just general inflammation? What specifically about their structure is stimulating the required inflammation needed for TLS formation? In terms of therapeutic efficacy in their models, are the TLS contributing to response? Or simply a surrogate of the other immune effects and more a bystander?*"

Response 11:

Thanks for the reviewer's valuable suggestion. Actually, the mechanisms underlying TLS formation are not fully understood, but existing studies suggest that TLS formation is primarily related to the release of chemokines and inflammatory factors in the tumor microenvironment. Notably, mature dendritic cells secrete CCL19 and CCL21, while $CD4^+$ T cells secrete CXCL13. These cytokines play a crucial role in the formation of T cell zones and

B cell zones within TLS. In this study, we believe that AIE COF-mediated phototherapy elevated the levels of inflammatory factors within the tumor. These inflammatory factors are essential for the infiltration and expansion of T cells and B cells. Additionally, AIE COF-mediated phototherapy promotes the maturation of dendritic cells, further facilitating the migration of T cells and B cells into the tumor, thereby forming T cell and B cell zones.

Regarding the issue of TLS and response to ICB therapy. First, we apologize for not explaining the relationship between TLS and ICB therapy response rate in the discussion section. We have already added this part of the content in the revised discussion section. Existing studies have confirmed the relationship between the presence of TLS and the response to ICB therapy. These findings also suggest that the presence of TLS is a better predictor of ICB efficacy than the degree of intratumoral immune infiltration.

Revision made:

We have added more content in the revised discussion section and highlight in BLUE in the revised manuscript (page 21, line 18 to 33) with details as following:

Previous studies have demonstrated that tumor cells release inflammatory cytokines such as TNFα, IFNγ, and CXCL10 under stress conditions.[69-71] In this study, we found that the AIE COF-mediated phototherapy effectively promotes the release of these inflammatory factors by inducing thermal and chemical damage directly to the tumor cells. These dying tumor cells can then act as an in situ vaccine, activating DCs. Subsequently, mature DCs secrete cytokines such as CCL19 and CCL21, to facilitate the recruitment of T cells and B cells into the tumor, allowing the formation of T cell zones and B cell zones within the TLS.[72-73] Furthermore, the inflammatory cytokines secreted by tumor cells, including CXCL10, TNFα, IFNγ, and IFNβ, promote the localization and maturation of T lymphocytes within the TME.[69] We also confirmed increased intratumoral T cell infiltration using scRNA-seq and flow cytometry analysis. Our scRNA-seq data validated that this increase in T cell content was accompanied by elevated levels of T cell-associated cytokines, such as IL22, IL7, and IL13, which are essential for B cell maturation and proliferation.[74-76] In addition, the mIHC results also unveiled that mature dendritic cells and dying tumor cells, along with inflammatory cytokines, facilitate the recruitment and proliferation of B cells and T cells, ultimately forming B cell and T cell clusters within the TLS.

Reviewer #3:

Comments:

This manuscript has described a AIEgens-based covalent organic frameworks (COFs) with PDT and PTT therapeutic effects for the modulation of anti-tumour immune response. Utilizing the AIEgens-based COFs to promote the formation of tertiary lymphoid structures (TLS) to tune the anti-tumour immune response provides a new direction for future cancer immunotherapy. To further improve the quality of the manuscript for publication in Nature Communications, some concerns should be addressed.

Response:

We would like to thank the reviewer for the positive and constructive comments. We also highly appreciate the reviewer's suggestion for strengthening our work. We have performed more experiments to address the reviewer's concerns. By responding to the reviewer's comments in detail and revising the manuscript accordingly, we believe this manuscript has been strengthened. All revisions are highlighted in BLUE color in the revised manuscript and Supplementary Information.

Comment 1:

1. "*In figure 4 f and I, how the authors decided the irradiation power and time?*"

Response 1:

We sincerely thank the reviewer for their careful reading. The suitable irradiation power and time is mainly based on our previous experience, we apologize for not systematically determining the irradiation time and power density, and we will address this more rigorously in our future studies. In this work, the irradiation time was set to 5 minutes, consistent with our previously reported protocols (*Nat. Commun.* **14**, 5355 (2023)). Given the suboptimal PTT performance of these COFs, we selected a power density of 1.0 W cm^{-2}, which is the maximum output of the 660 nm laser, to achieve enhanced PTT efficacy.

Comment 2:

2. "*The suitable particle size and water dispersity is one of the most important challenges for the application of COF as biomedical materials, thus, it would be more complete if the authors provide more information on the morphology related properties of COFs, such as size stability, size distribution of COFs in physiological environment.*"

Response 2:

We thank the reviewer for raising this important concern. As suggested, we tested the stability and size distribution of TPDA-ViBT-COF in different solvents. The results indicated that the size distributions of TPDA-ViBT-COF in various solvents, such as water, PBS, and EtOH, are very similar, demonstrating the stability of TPDA-ViBT-COF in different physiological environments. We also assessed the size stability of TPDA-ViBT-COF over different time intervals, including 6 h, 12 h, and 24 h. The particle size of TPDA-ViBT-COF significantly increased from 190 nm to several micrometers over time. This may be attributed to the

inherent aggregation property of COF materials. Despite sonication into nano-sized particles, these COF materials tend to re-aggregate into micro-sized particles. Inspired by the reviewer's insightful comment, we believe that wrapping the COF surface with a cell membrane may address its inherent aggregation tendency, and we plan to investigate this approach in the future.

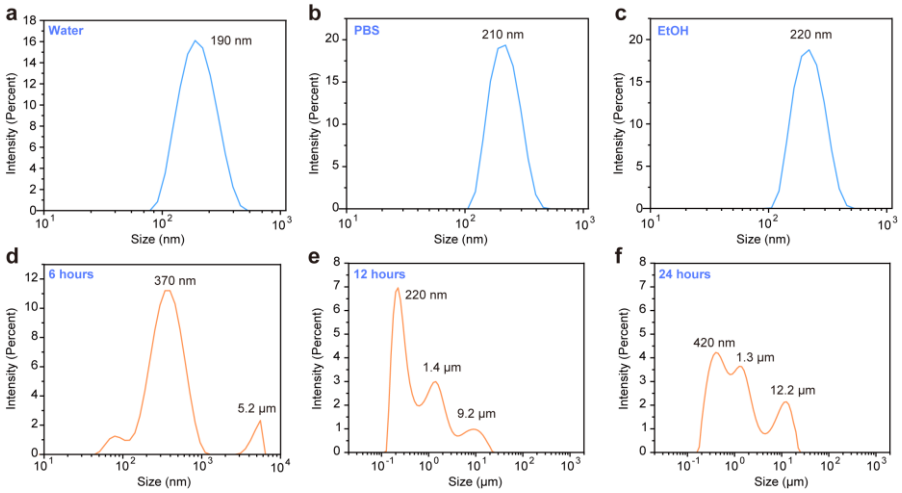

Fig. R20. Stability and size distributions of TPDA-ViBT-COF in different solvents and over different time.

Comment 3:

3. "*As showed in figure 4 g, the TPDA-ViBT-COF showed an ellipse structure with a size of 180 nm, is the TPDA-TDTA-COF, TPDA-BT-COF showed a same size range and morphology, is there any relationship between the size, morphology and its PDT, PTT properties.*"

Response 3:

We thank the reviewer for their constructive suggestion. As recommended, we characterized the morphology and particle size of TPDA-TDTA-COF and TPDA-BT-COF. As shown in Fig. R21, the morphologies of TPDA-TDTA-COF and TPDA-BT-COF are similar to that of TPDA-ViBT-COF but exhibit a thicker morphology. Additionally, the particle size of TPDA-BT-COF is larger compared to TPDA-ViBT-COF. We strongly agree with the reviewer's insightful comment regarding the relationship between size, morphology, and phototherapy performance. The particle size and morphology of nanomedicines can significantly influence their cellular uptake and tissue dispersion efficiency, which is critical for realizing their biological functionality (*ACS Nano*. **13**, 9542019, (2019)). Unfortunately, precise control over the particle size and morphology of COF materials remains challenging. We will endeavor to address this critical issue in our future studies.

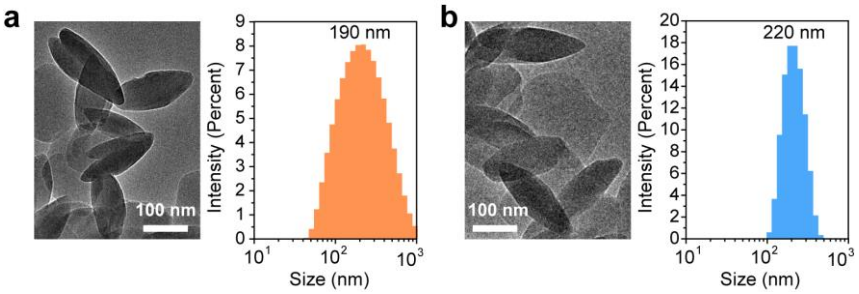

Fig. R21. (**a**) TEM images and particle size distribution of TPDA-TDTA-COF. (**b**) TEM images and particle size distribution of TPDA-BT-COF.

Comment 4:

4. "*In figure 4, the authors showed excellent phototoxicity towards cancer cells, it would be more complete if the authors carry out more detailed studies on the phototoxicity on other cell types, such as immune cells, epithelial cells and stromal cells.*"

Response 4:

Thanks for the reviewer's valuable suggestion. As the reviewer suggested, we evaluated the cytotoxicity of TPDA-ViBT-COF with or without laser on L929 (stromal cells), RAW264.7 (immune cells) and HOK (epithelial cells) cells. The results indicated that, in comparison to MC38 cells, TPDA-ViBT-COF+Laser exhibited lower toxicity in L929, RAW264.7 and HOK cells.

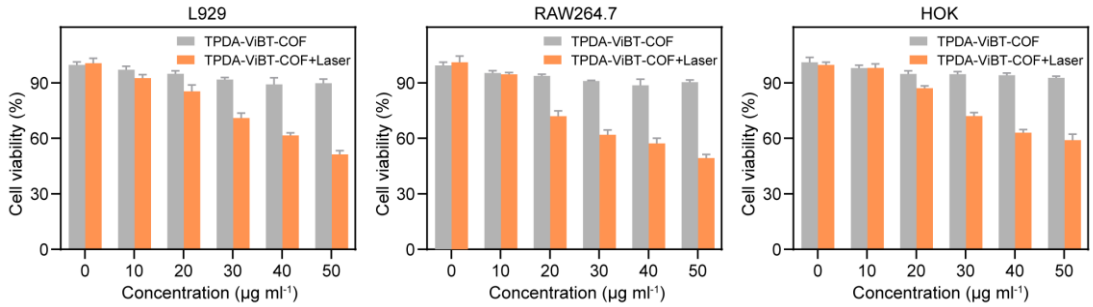

Fig. R22. Cytotoxicity of TPDA-ViBT-COF without (h) or upon 660 nm laser irradiation for L929, RAW264.7 and HOK cells.

Revision made:

We have added data of Fig. R22 as "Supplementary Fig. 13." in the revised Supplementary Materials and highlight in BLUE on page 22.

Comment 5:

5. "*In supplementary fig 11, the authors showed the internalization of COFs into MC38 cells, it would be more complete if the authors can locate the subcellular organelle that the COFs in.*"

Response 5:

Thanks for the reviewer's constructive suggestion. As the reviewer suggested, we labeled lysosomes (LAMP1), mitochondria (HSP60), and the endoplasmic reticulum (GRP94) with their respective biomarkers. Through confocal microscopy, we observed that the red fluorescence signal of COF co-localized with lysosomes and the endoplasmic reticulum but not with mitochondria. These results indicate that COF is mainly distributed within the

lysosomes and endoplasmic reticulum of the MC38 cells.

Revision made:

We have added Fig. R23 as "Supplementary Fig. 12." in the revised Supplementary Materials, with details as following:

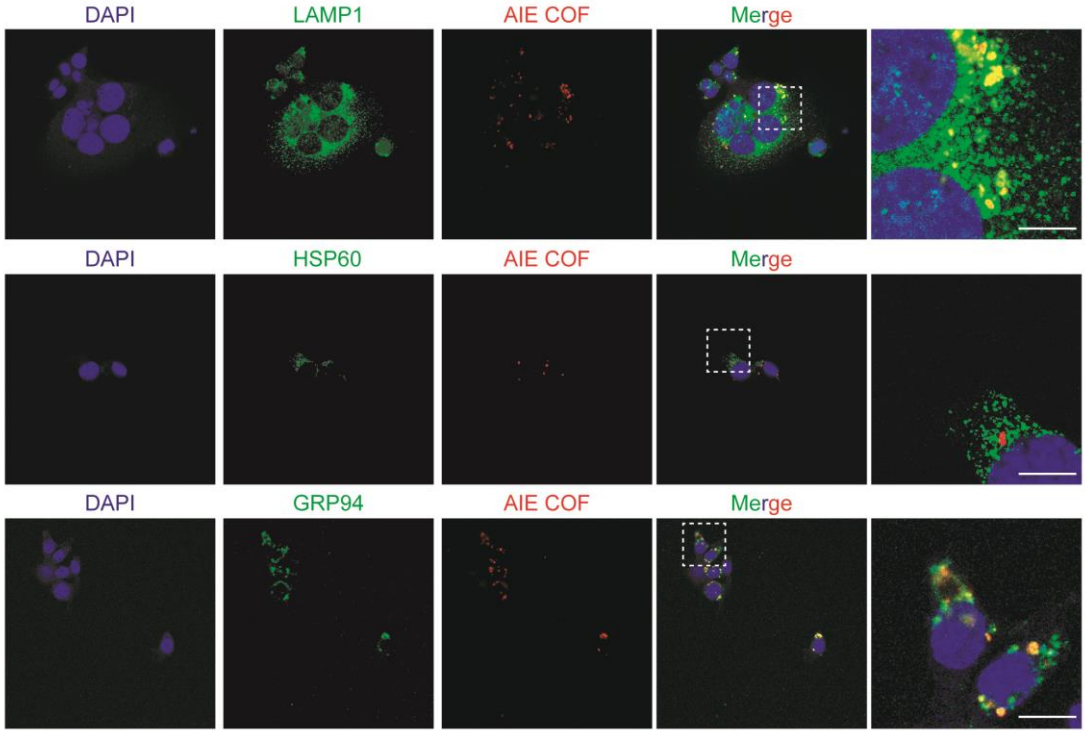

Fig. R23. Subcellular distribution of AIE COF in MC38 cell, scale bar = 10 μm.

Comment 6:

6. "*It would be more comprehensive if the authors carry out in vitro studies to show the activation of immune cells, such as maturation of DCs, polarization of macrophages as well as the proliferation and activation of T cells after treatment with AIE-COFs with cancer cells.*"

Response 6:

We thank this reviewer for the valuable suggestion. Based on the reviewer's suggestion, we added the effects of AIE COFs on tumor cell-induced macrophage polarization and DCs maturation. When AIE COF-treated MC38 cells were co-cultured with primary DCs, the expression of CD80 and CD86 in dendritic cells increased, indicating activation and maturation of dendritic cells. When co-cultured with RAW264.7 cells, the expression of CD206 on the surface of RAW264.7 cells decreased while CD86 expression increased, indicating that AIE COF-treated MC38 cells can promote M1 macrophage polarization.

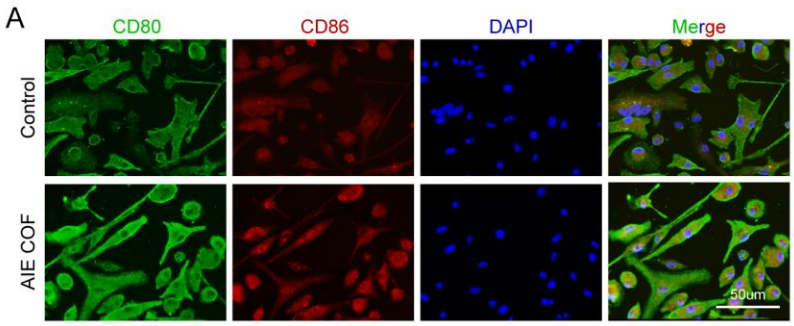

Fig. R24. Representative images of CD80 and CD86 immunofluorescence staining of primary DCs co-culture with TPDA-ViBT-COF treated MC38 cells, scale bar = 50 μm.

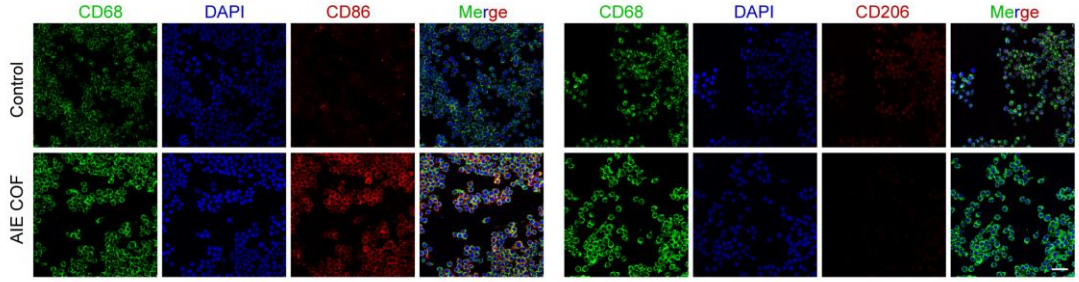

Fig. R25. Representative images of CD68, CD86 and CD206 immunofluorescence staining of RAW26.4 cells co-culture with TPDA-ViBT-COF treated MC38 cells, scale bar = 50 μm.

Revision made:

We have added Fig. R25 as "Supplementary Fig. 25." in the revised Supplementary Materials.

Comment 7:

7. "*The biodistribution of COFs in tumor essentially its uptake by immune cells such as DCs, macrophages as well as T cells is an important question to answer considering the extreme cell cytotoxicity of COFs under laser irradiation. Thus, it would be more comprehensive if the authors can provide data on the distributions of COFs in tumors.*"

Response 7:

We thank the reviewer for this constructive suggestion. According to the reviewer's suggestion, we investigated the distribution of AIE COFs within the tumor by staining consecutive sections of tumor tissue. We found that AIE COFs was scattered throughout the tumor, but we did not observe AIE COFs in the T cell and dendritic cell regions. Although macrophages were present in high quantities in the tumor, very few were located in the areas where AIE COFs were distributed.

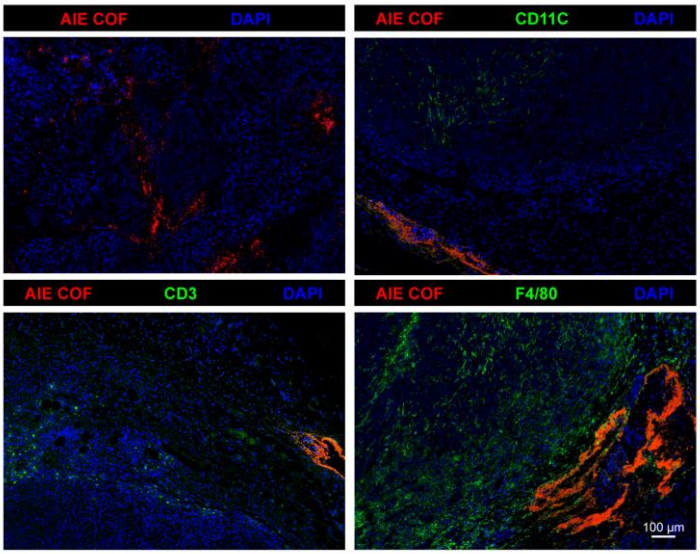

Fig. R26. The distributions of AIE COFs in tumor, scale bar = 100 μm.

Comment 8:

8. "*Why the authors choose intratumorally administration way? It would be more complete if the authors can carry out more studies on the impact of administration way of COFs on its therapeutic effects, such as i.v. injection.*"

Response 8:

We thank the reviewer for this constructive suggestion. As descripted in comment 2, even after sonication into nano-sized particles, these COF materials is tending to re-aggregate into micro-sized particles within several hours, thus hardly used by intravenous injection. Inspired by the reviewer's insightful comment, we believe that wrapping the COF surface with a cell membrane may address its inherent aggregation tendency, and we plan to investigate this approach in the near future.

Comment 9:

9. "*As showed in figure 5, after treatment with COFs, including TPDA-TDTA-COF, TPDA-BT-COF, and TPDA-ViBT-COF showed a 30% to 70% complete tumor eradication. Besides, it showed a higher level of TCM and TEM, T, thus, it would be more complete if the authors can carry out a detailed tumor rechallenge studies.*"

Response 9:

We thank the reviewer for their valuable suggestion. According to the reviewer's suggestion, we carried out a more detailed tumor rechallenge experiment with 4 groups including: control, TPDA-TDTA-COF+aCTLA4, TPDA-BT-COF+aCTLA4, and TPDA-ViBT-COF+aCTLA4. The results demonstrated that mice treated with TPDA-ViBT-COF+aCTLA4 exhibited no detectable tumor recurrence, whereas untreated mice experienced significant tumor recurrence. Additionally, mice treated with TPDA-TDTA-COF+aCTLA4 and TPDA-BT-COF+aCTLA4 exhibited only partial inhibition of tumor recurrence, without complete prevention.

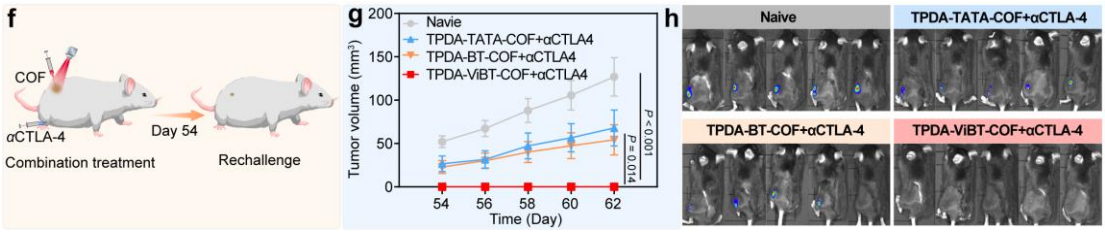

Fig. R27. (**f**) The treatment protocol of rechallenge experiments. (**g**) The growth curve of tumors in the control, TPDA-TDTA-COF+aCTLA4, TPDA-BT-COF+aCTLA4, and TPDA-ViBT-COF+αCTLA4, n = 6 independent samples. (**h**) Bioluminescence images of mice in the naïve, TPDA-TDTA-COF+aCTLA4, TPDA-BT-COF+aCTLA4, and TPDA-ViBT-COF+αCTLA4, n = 6 independent samples.

Revision made:

We have added Fig. R27 as "Fig. 9f to 9h." in the revised manuscript.

Comment 10:

10. "*In figure 5, the authors showed the changes on population of major immune cells in spleen and TDLN. It would be more direct if the authors carry out studies of the infiltration of immune cells inside the tumors as well as its activation.*"

Response 10:

We thank the reviewer for their valuable suggestion. As recommended, we assessed immune cell infiltration and activation within the tumor. The results revealed an increased proportion of T cells following treatment with TPDA-ViBT-COF+laser, indicating that TPDA-ViBT-COF+laser treatment may promote T cell clonal expansion. Additionally, we observed an increase in $CD4^+$ effector memory T cells (T_{EM}) cells in the TPDA-ViBT-COF+laser treated tumors, while the proportion of immunosuppressive myeloid-derived suppressor cells (MDSCs) was markedly decreased.

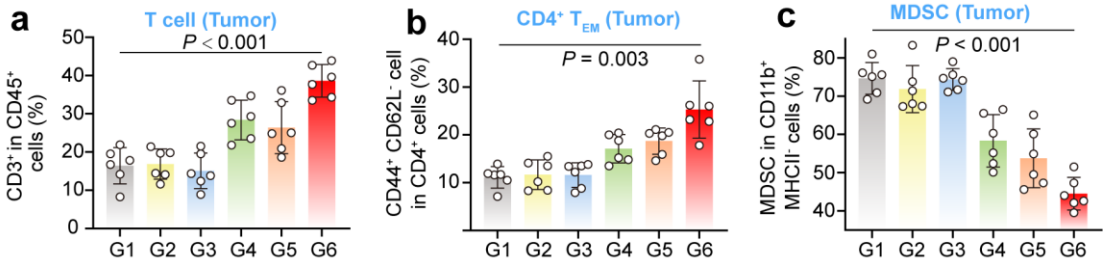

Fig. R28. (a) Quantification of T cell ($CD3^+$) gating on $CD45^+$ cells in tumor, n = 6 independent samples. (b) Quantification the gating of $CD4^+$ T_{EM} ($CD44^+CD62L^-$) on $CD3^+$ $CD4^+$in tumor, n = 6 independent samples. (c) Quantification of MDSC ($Ly6G^{high}$ $Ly6C^{low}$) gating on $CD11b^+$ $MHCII^-$ cells in the spleen, n = 6 independent samples. G1: Control; G2: Laser; G3: TPDA-TPDA-COF; G4: TPDA-TPDA-COF+660 nm; G5: TPDA-BT-COF+660 nm; G6: TPDA-ViBT-COF+660 nm.

Revision made:

We have added Fig. R28 as "Fig. 5." in the revised manuscript.

Comment 11:

11. "*In figure 6, the authors showed that, after treatment with COFs, the proportion of epithelial and stromal cell was sharply reduced, it would be more comprehensive if the authors can provide a possible explanation for such impact of COFs on those cells.*"

Response 11:

Thanks for the reviewer's insightful comment. The epithelial and stromal cells in the tumor mainly consist of tumor cells and tumor-associated fibroblasts. The decrease in the proportion of tumor cells and fibroblasts primarily attributed to the cytotoxic effect of TPDA-ViBT-COF-mediated phototherapy reducing the proportion of tumor cells. Additionally, the release of tumor antigens and inflammatory cytokines increases the infiltration of immune effector cells. The reduction in the tumor and stromal cells ratio, combined with the increase in immune cell proportion, collectively may leads to a decrease in the proportion of non-immune cells.

Revision made:

In the revised manuscript, we have added a possible explanation for the decrease in the ratio of epithelial and stromal cell, with details as following:

This may be attributed to the cytotoxic effect of TPDA-ViBT-COF-mediated phototherapy reducing the proportion of tumor cells. Additionally, the release of tumor antigens and inflammatory cytokines increases the infiltration of immune effector cells. The reduction in the tumor and stromal cell ratio, combined with the increase in immune cell proportion, collectively leads to a decrease in the proportion of non-immune cells.

Comment 12:

12. "*As showed in figure 6 e, after treatment with COFs, the proportion of Tregs was increased comparing with untreated group, why the PTT and PDT therapy have an impact on Tregs.?*"

Response 12:

We appreciate the reviewer's constructive suggestion. While PDT and PTT effectively kill tumor cells, they also induce the release of pro-inflammatory cytokines such as IFNγ and TNFα. This was also confirmed by our ELISA data (Fig. R29), where the levels of these cytokines are elevated after treated by COF-mediated PDT and PTT. Moreover, this increase promotes the maturation of $CD4^+$ T cells, which often leads to an upsurge in Treg differentiation (*Immunity* **56**, 386-405(2023)).

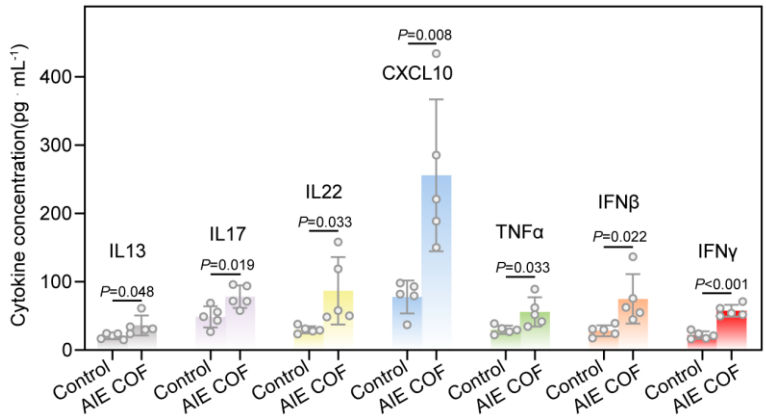

Fig. R29. Quantification of the levels of various cytokines and chemokines in tumors following treatment with control or TPDA-ViBT-COF, n = 5 independent samples.

Comment 13:

13. "*Is there any difference on the PD-L1 expression on the tumors after treatment? why the combinational treatment with CTAL-4 antibody is better than PD-1 antibody?*"

Response 13:

We thank the reviewer for their valuable suggestion. In accordance with the reviewer's recommendation, we examined the expression of PD-L1 on the surface of tumor cells after treatment with TPDA-ViBT-COF+Laser (please see Fig. R30). Flow cytometry analysis revealed that, in comparison to the control group, there is no significant difference in PD-L1 expression on $CD45^-$ cells in tumor tissues treated with TPDA-ViBT-COF+Laser. Additionally, multiplex immunohistochemistry results corroborated these findings, showing no apparent change in PD-L1 expression on the surface of tumor cells after TPDA-ViBT-COF+Laser treatment.

Regarding the reason for the superior efficacy of combining CTLA-4 blockade with TPDA-ViBT-COF+Laser treatment, we utilized the CellPhoneDB algorithm to analyze immune inhibitory receptor-ligand interactions within the tumor, as shown in Figure 8h. The results indicated that, compared to the PD1-PD-L1 interaction, the CTLA4-CD86 interaction is the most prevalent immune inhibitory receptor-ligand pair in tumor tissues treated with TPDA-ViBT-COF+Laser. We apologize for the inappropriate labeling of gene names in Figure 8h. In this figure, we used the aliases CD274 for PDL1 and PDCD1 for PD1 to label the genes, which are not the most widely recognized names. In the revised manuscript, we have corrected these labels to PDL1 and PD1, respectively. Given that CTLA4-CD86 is more prevalent than PDL1-PD1 in tumor tissues treated with TPDA-ViBT-COF+Laser, we hypothesized that CTLA4 blockade might be more effective than PD1 blockade. We subsequently validated this hypothesis through further animal experiments.

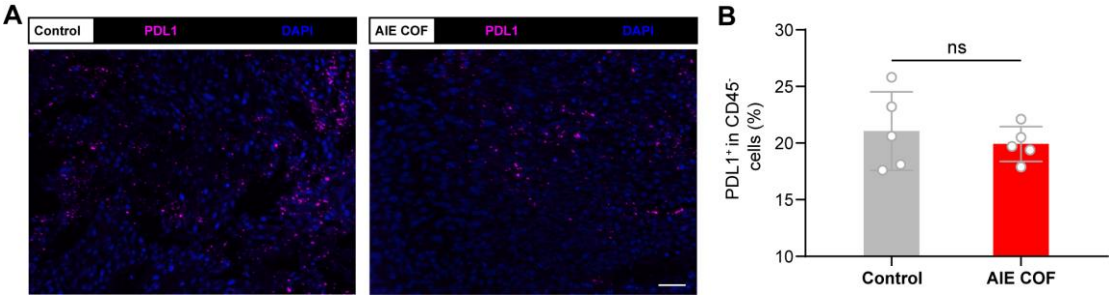

Fig. R30. (a) Immunofluorescence images of $PD\text{-}L1^+$ cells before and after treatment in tumor, scale bar = 50 μm. (b) Quantification of $PD\text{-}L1^+$ cells gating on $CD45^-$ cells in tumor, n = 5 independent samples.

Revision made:

We have added Fig. R30 as "Supplementary Fig. 31." in the revised Supplementary Materials.

Point-by-Point Response to Reviewers' Comments

Reviewers Comments:

==========

Reviewer #1:

Comments:

Thank you for your detailed responses and the thoughtful revisions you've made in addressing my comments. I appreciate the effort to clarify and improve various aspects of your manuscript.

Response:

We are very grateful to the reviewer for pointing out the novelty of our work. We also highly appreciate the reviewer's careful reading and constructive suggestions that helped us to further the quality. By responding to the reviewer's comments in detail and revising the manuscript accordingly, we believe our manuscript has been significantly strengthened. All revisions are highlighted in BLUE color in the revised manuscript and Supplementary Information.

Comment 1:

1. *"Overall, your revisions have addressed my comments comprehensively, and the manuscript is much improved as a result. I believe these changes have significantly strengthened your work, and I have no further major concerns. However, I encourage you to ensure that all statistical data is clearly presented, as consistent and transparent data presentation is crucial for maintaining scientific rigor."*

Response 1:

We sincerely appreciate the reviewer's positive feedback and acknowledgment of the improvements made to the manuscript. We fully agree on the importance of presenting all statistical data clearly to ensure scientific rigor. In response to the reviewer's suggestion, we have thoroughly reviewed the manuscript to ensure that all results with statistically significant differences are clearly indicated and appropriately labeled. We hope these updates fully address the reviewer's comments and enhance the clarity of our data presentation. Thank you again for your valuable insights. Relevant statistical annotations have been added to each figure where applicable with details as the following:

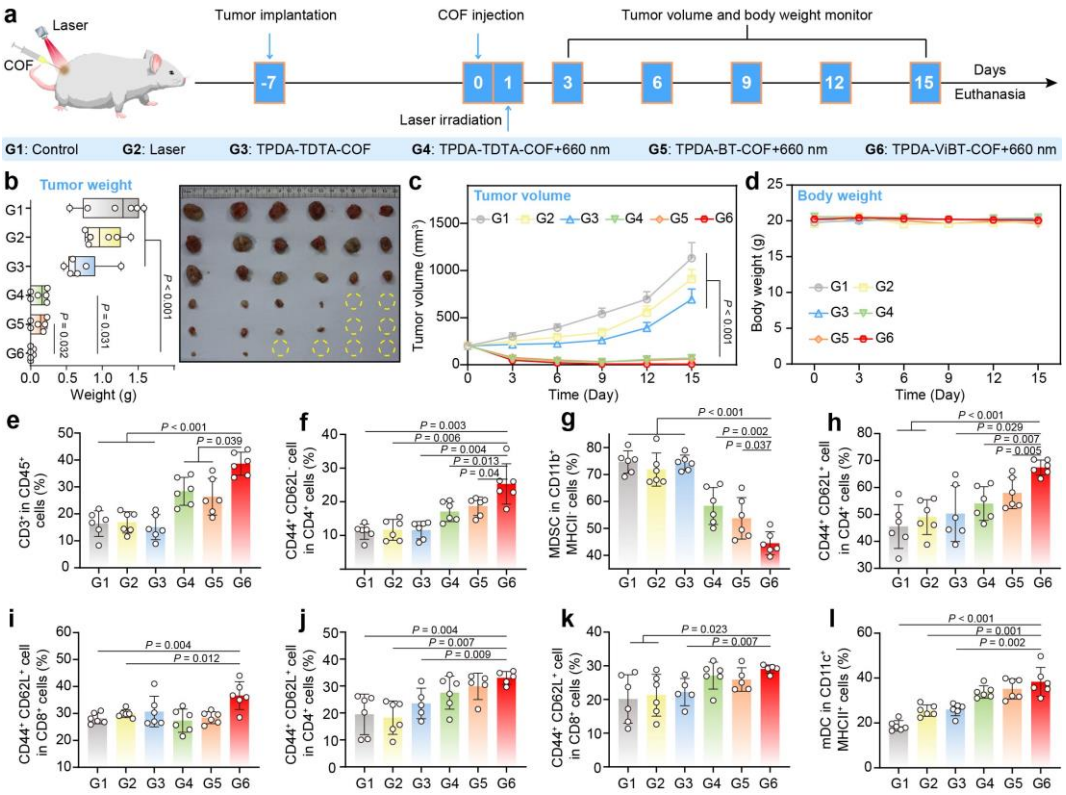

Fig. 5. Antitumor effects of TPDA-TDTA-COF, TPDA-BT-COF and TPDA-ViBT-COF in a MC38 tumor-bearing mice model. (a) The treatment protocol of AIE COF-mediated antitumor effects. (b) The images and the weight of MC38 tumors on day 15. Tumor volume (c) and body weights (d) of MC38 tumor-bearing mice, n = 6 independent samples. (e) Quantification of T cell ($CD3^+$) gating on $CD45^+$ cells in tumor, n = 6 independent samples. (f) and (g) Quantification of $CD4^+$ T_{EM} ($CD44^+CD62L^-$) and MDSC gating on $CD11b^+$ $MHCII^-$ cells in tumor, n = 6 independent samples. (h to k) Quantification the gating of $CD4^+$ T_{CM}/$CD8^+$ T_{CM} ($CD44^+CD62L^+$) on $CD3^+$ $CD4^+$/ $CD8^+$ in both TDLN and spleen, n = 5-6 independent samples. (l) Quantification of mDC in the TDLN, n = 6 independent samples. Data are presented as mean ± SEM, and statistical significance was assessed using two-tailed Student's t-test, one-way ANOVA with post hoc Tukey test was used when comparing more than two groups. Source data are provided as a Source Data file.

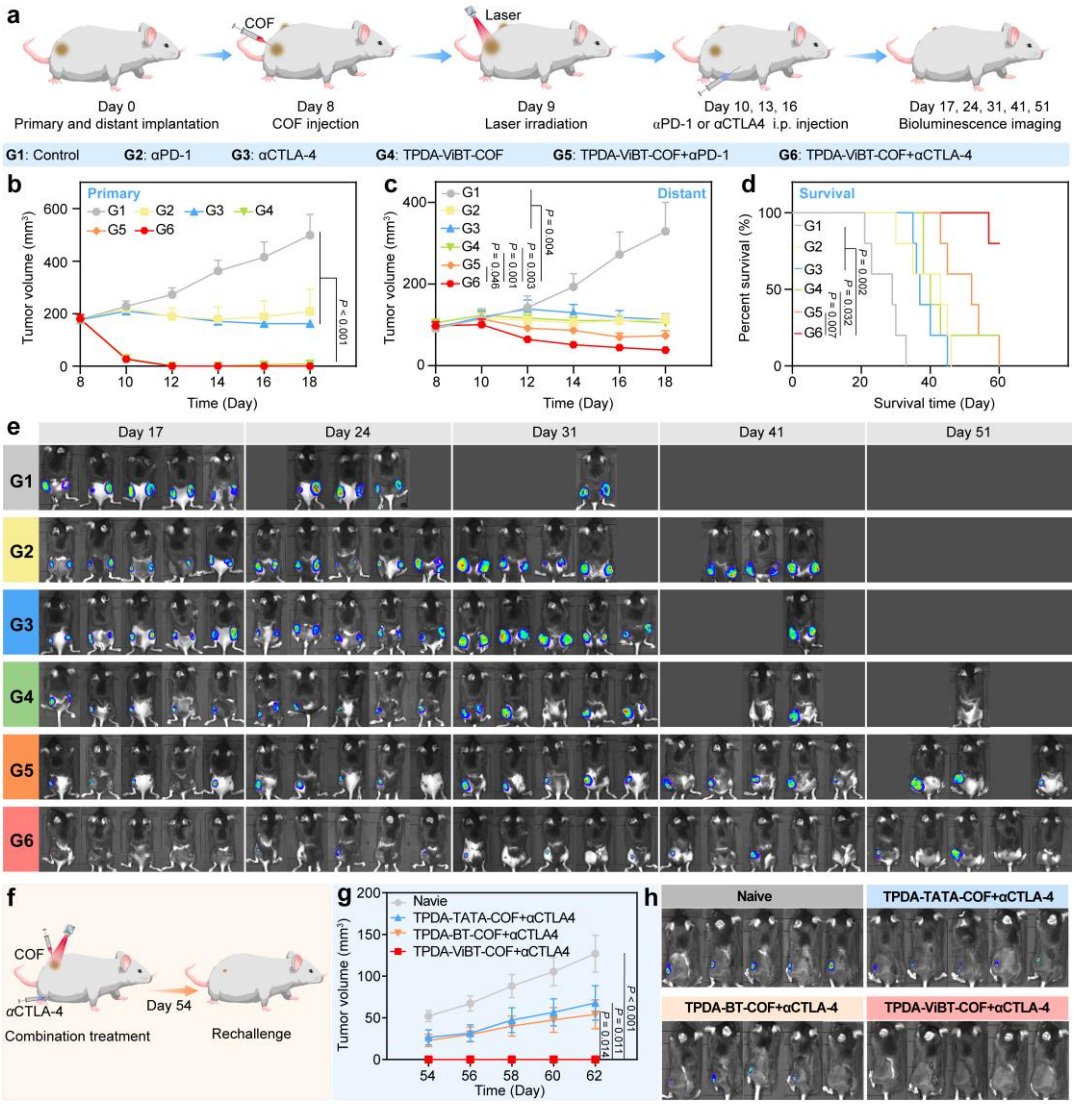

Fig. 9. TPDA-ViBT-COF-mediated ICB. (**a**) Schematic illustration of the combination therapy of TPDA-ViBT-COF+αCTLA4. The tumor growth curves of primary (**b**) and distant (**c**) and the percentage of survival (**d**) among MC38 mice following various treatments, n = 5 independent samples. (**e**) Bioimages of MC38 mice following various treatments. (**f**) The treatment protocol of rechallenge experiments. (**g**) The growth curve of tumors in the control, TPDA-TDTA-COF+αCTLA4, TPDA-BT-COF+αCTLA4, and TPDA-ViBT-COF+αCTLA4, n = 6 independent samples. (**h**) Bioluminescence images of mice in the naïve, TPDA-TDTA-COF+αCTLA4, TPDA-BT-COF+αCTLA4, and TPDA-ViBT-COF+αCTLA4, n = 6 independent samples. Data in this study are presented as mean ± SEM, and statistical significance was determined by performing two-tailed Student's t-test, one-way ANOVA with post hoc Tukey test was used when comparing more than two groups. Survival analysis was conducted using the log-rank Mantel-Cox test. Source data are provided as a Source Data file.

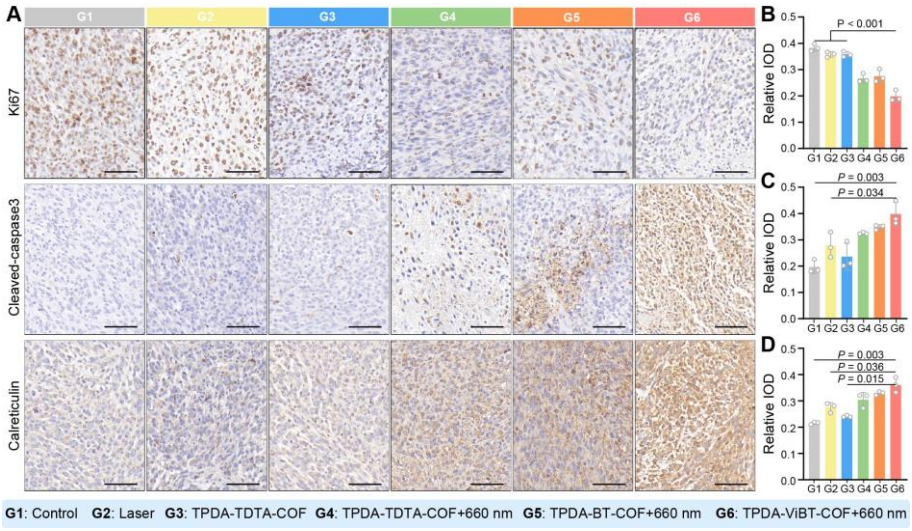

Supplementary Fig. 14. Quantification and representative immunohistochemical images of Ki67, Cleaved Caspase-3, and Calreticulin under different treatments, scale bar = 50 μm. n = 3 independent samples Source data are provided as a Source Data file.

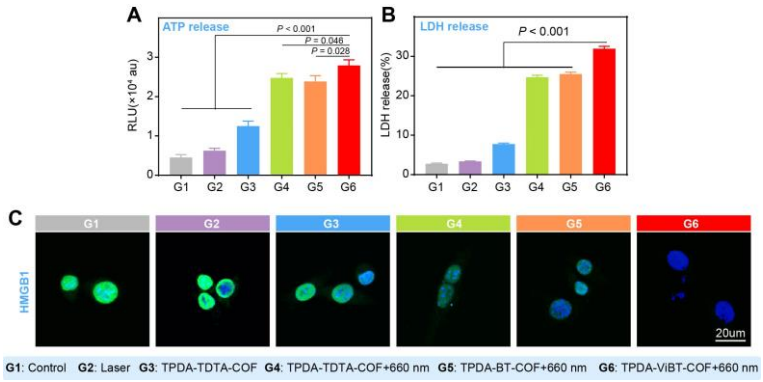

Supplementary Fig. 15. ATP (**A**) andLDH (**B**) in MC38 cells after various treatments; data are presented as mean ± SEM (n = 3 independent samples). **C**, Representative images of HMGB1 immunofluorescence staining in MC38 cells after treatment with different samples. Source data are provided as a Source Data file.

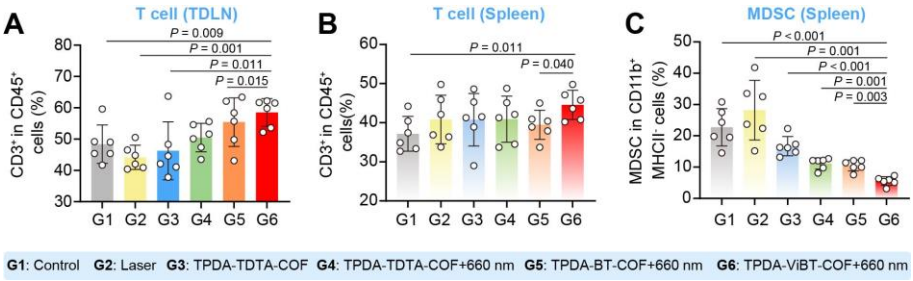

Supplementary Fig. 20. (A) Quantification of T cell ($CD3^+$) gating on $CD45^+$ cells in TDLNs, n = 6 independent samples. (B) to (C) Quantification of T cell ($CD3^+$) gating on $CD45^+$ cells in Spleen, n = 6 independent samples. Quantification of MDSC ($Ly6G^{high}$ $Ly6C^{low}$) gating on $CD11b^+$ $MHCII^-$ cells in the spleen, n = 6 independent samples. Source data are provided as a Source Data file.

Reviewer #2:

Comments:

Zhang et al. re-submitted manuscript titled 'Trigger inducible tertiary lymphoid structure formation using covalent organic frameworks for cancer immunotherapy' in which they develop an artificial covalent organic framework for intra-tumor injection to induce tertiary lymphoid structure and anti-tumor immunity. The strength of this article is in optimizing this artificial nanostructure and its photothermal effects in inducing these effects. They have carefully and thoughtfully addressed the concerns expressed by myself as well as the other 2 reviewers to the best of their abilities. The figures and text read clearer with clearer descriptions and explanations of abbreviations. Required details on methodology and adjustment of flow analyses have also strengthened the manuscript. A few additional comments below:

Response:

We are very grateful to the reviewer for their careful reading and pointing out the novelty of our work. We also highly appreciate the reviewer's suggestion for strengthening our work. By responding to the reviewer's comments in detail and revising the manuscript accordingly, we believe that our manuscript has been significantly strengthened. All revisions are highlighted in BLUE color in the revised manuscript and Supplementary Information.

Comment 1:

1. "*Figure 7e - the labels on top PNAD, CD3, etc. don't seem to necessarily be in the same order in the single color stains below the multiplexed figure This should be corrected. This should be checked in all multiplexed figures.*"

Response 1:

Thank you for your careful review and valuable feedback on Figure 7e. We have thoroughly examined the figure and agree that the labels (e.g., PNAD, CD3, etc.) were not in the same order as the single-color stains below the multiplexed figure. We have corrected this in Figure 7e to ensure the labels are consistent with the single-color stains. Additionally, we have reviewed all other multiplexed figures to verify that the labeling order is accurate.

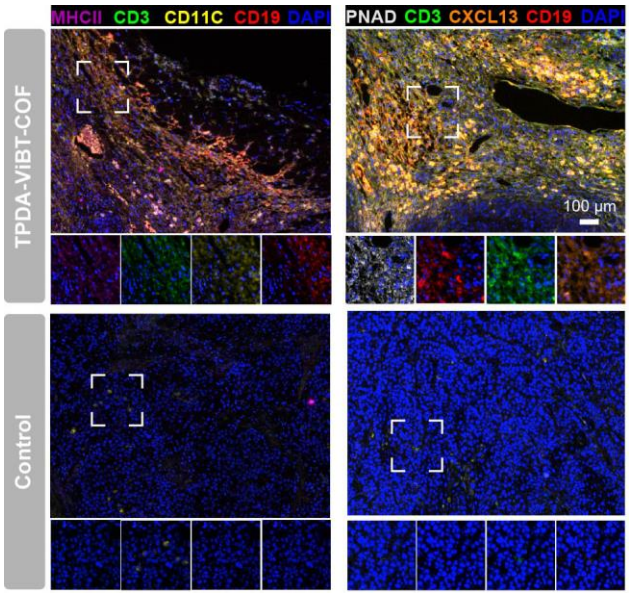

Fig 7e. Representative images of mIHC staining of MHCII (purple), CD3 (green), CD11C (yellow), CD19 (red), PNAD (white), CXCL13 (orange), and DAPI (blue) in 4MOSC1 tumor with or without TPDA-ViBT-COF treatment, scale bar = 100 μm.

Comment 2:

2. "*Response to my 2nd comment on benefit of their methodology to induce TLS compared to others and limitations that it is not effective in cold tumors is significant. The inability to not induce in a cold tumor is a limitation in significance of this. It is not clear in their response that they included this in the manuscript and should include this limitation and discussion in the manuscript.*"

Response 2:

We appreciate the reviewer's insightful comment regarding the limitation of our methodology in cold tumors. We agree that the inability to induce TLS in cold tumors is a significant limitation of our current approach. Although our study demonstrated the successful formation of TLS in hot tumors, we did not observe the same efficacy in cold tumor models, where the immune microenvironment lacks pre-existing immune cell infiltration. We will revise the manuscript to explicitly include this limitation. Specifically, we will highlight that further optimization is necessary to adapt AIE COF-mediated phototherapy for cold tumors, such as Chimeric Antigen Receptor T-Cell Immunotherapy or other treatments to recruit immune cells and prime the tumor microenvironment for TLS formation.

Revision made:

In the revised manuscript, we have added a discussion in the manuscript regarding the limitation of AIE COF in failing to induce TLS formation in cold tumors, as well as potential solutions for addressing this issue in the future, with details as following:

Additionally, our method showed limited efficacy in cold tumors, where immune cells are not naturally present within the tumor microenvironment, making TLS induction more

challenging. This limitation suggests that combining AIE COF therapy with other immune-modulating strategies, such as Chimeric Antigen Receptor T-Cell Immunotherapy, may be necessary to trigger TLS formation in such contexts.

Reviewer #3:

Comments:

This manuscript has described a AIEgens-based covalent organic frameworks (COFs) with PDT and PTT therapeutic effects for the modulation of anti-tumour immune response. Utilizing the AIEgens-based COFs to promote the formation of tertiary lymphoid structures (TLS) to tune the anti-tumour immune response provides a new direction for future cancer immunotherapy. To further improve the quality of the manuscript for publication in Nature Communications, some concerns should be addressed.

Response:

We would like to thank the reviewer for the positive and constructive comments. We also highly appreciate the reviewer's suggestion for strengthening our work. We have performed more experiments to address the reviewer's concerns. By responding to the reviewer's comments in detail and revising the manuscript accordingly, we believe this manuscript has been strengthened. All revisions are highlighted in BLUE color in the revised manuscript and Supplementary Information.

Comment 1:

1. "*Several statements in the caption of figure1 should be further clarified, such as "the analysis indicated that αPD-1 expression in T cells….", "a ligand for αCTLA4".*"

Response 1:

We sincerely thank the reviewer for their careful reading and valuable suggestions. We acknowledge the misuse of the terms "αPD-1" and "αCTLA4" in the original figure caption. The correct terms should be "PD-1" (programmed cell death protein 1) and "CTLA-4" (cytotoxic T-lymphocyte-associated protein 4), as they refer to the receptors themselves rather than their respective blocking antibodies. We will revise the manuscript accordingly to ensure accurate terminology. This correction will be reflected in the revised figure caption for clarity and accuracy.

Revision made:

In the revised manuscript, we have rephrased the description for Figure 1 in the Figure legend with details as the following:

Fig. 1 Illustration of the design of scRNA-seq aided immunotherapy facilitated by AIE COF-induced TLS formation. The application of AIE COF-mediated phototherapy leads to the induction of TLS formation by stimulating the excessive secretion of key cytokines. This process subsequently promotes the maturation, proliferation, and migration of T and B cells. To explore the underlying mechanisms, single-cell sequencing was utilized, and receptor-ligand interactions between cells were analyzed using CellphoneDB, a tool for characterizing cell-cell communication networks from scRNA-seq data. Notably, the analysis indicated that PD-1 expression in T cells did not obviously increase following AIE COF treatment. In contrast, there of CD86 expression, a ligand for CTLA4, was markedly

upregulated. Consequently, combining αCTLA4 blockade with AIE COF treatment exhibits a higher potential to effectively suppress the growth of both primary and distant tumors.

Comment 2:

2. "*In the revised manuscript, the authors showed that the AIE-COFs showed a greater toxicity to cancer cell line than other cell types, it would be more comprehensive if the authors provide a possible explanation for this selectivity of AIE-COFs to cancer cells.*"

Response 2:

We appreciate the reviewer's insightful suggestion. The selective toxicity of AIE-COFs to cancer cells may be attributed to the inherent differences in the redox states between cancerous and normal cells. Cancer cells exhibit elevated levels of ROS due to their dysregulated metabolic pathways, which makes them more vulnerable to further oxidative stress (*Redox Biol.* **2**, 535-562 (2014); **36**, 101652 (2020)). AIE-COFs induce additional ROS generation through phototherapy, exacerbating the oxidative stress specifically in cancer cells, leading to their selective cytotoxicity. Normal cells, on the other hand, have more robust antioxidant defense mechanisms, which help them neutralize ROS more effectively, thereby reducing the toxicity of AIE-COFs in non-cancerous cells (*Nat. Rev. Drug Discov.* **23**, 583-606 (2024)).

Revision made:

In the revised manuscript, we have provided a detailed explanation for the selective toxicity of AIE-COFs to cancer cells with details as the following:

In contrast, less than 25% of MC38 cells survived after being subjected to TPDA-ViBT-COF upon laser irradiation. In comparison to MC38 cells, TPDA-ViBT-COF combined with laser irradiation exhibited lower toxicity to L929 and HOK cells (Fig. 4i, Supplementary Fig. 13). This reduced toxicity in non-tumor cells can be attributed to their lower baseline levels of ROS and more robust antioxidant defense systems, which enable them to better manage oxidative stress induced by phototherapy. However, cancer cells, like MC38, typically exhibit elevated ROS levels and compromised antioxidant defenses, making them more susceptible to the oxidative damage triggered by AIE-COF-mediated phototherapy. This difference in cellular responses underpins the selective cytotoxicity observed in cancer cells.

Comment 3:

3. "*In the revised manuscript, the authors showed that the AIE-COFs mainly located in lysosomes and endoplasmic reticulum, is such distribution of AIE-COFs in MC38 cells can be observed in immune cells? Additionally, is such distribution further contributed to the excellent PDT and PTT effects on cancer cell lines. More importantly, it would be more*

complete if the authors provide detailed information on the interanimation pathways of AIE-COFs."

Response 3:

We thank the reviewer for their constructive suggestion. In response to the reviewer's question regarding the distribution of AIE-COFs in immune cells, we have supplemented our revised manuscript with additional data demonstrating the phagocytosis of AIE-COFs by RAW246.7 (macrophages). Through confocal microscopy, we observed that the red fluorescence signal of COF co-localized with lysosomes and the endoplasmic reticulum (ER) in RAW264.7 cells.

As for their localization in the ER, it is possible that AIE-COFs are trafficked to the ER following lysosomal escape. ER stress plays a critical role in inducing apoptosis in cancer cells by activating the unfolded protein response (UPR) pathway. Cancer cells are often more vulnerable to ER stress than normal cells due to their higher basal levels of ER stress (*Nat. Rev. Mol. Cell Biol.* **13**, 89-102 (2012)). Therefore, the ER localization of AIE-COFs could enhance their ability to disrupt protein folding and induce oxidative stress, thereby contributing to enhanced photodynamic therapy (PDT) and photothermal therapy (PTT) effects. Upon accumulation in lysosomes, AIE COFs, especially those with photosensitizing properties, can generate reactive oxygen species (ROS) under light irradiation, which causes oxidative stress. This oxidative damage can compromise the lysosomal membrane integrity, leading to its rupture (*J. Control Release.* **240**, 67-76 (2016)). The ensuing release of lysosomal enzymes, such as cathepsins, into the cytoplasm triggers apoptotic pathways, contributing to the effective eradication of tumor cells.

We agree with the reviewer’s comment that the interanimation pathways of AIE COFs is very important, and apologize for not investigating this aspect in the present study. Inspired by the reviewer’s valuable suggestion, we will conduct a comprehensive exploration of the interanimation pathway in our future research endeavors. Here, we proposed a potential interanimation pathways of AIE-COFs, drawing upon insights gleaned from antecedent nanomedicine investigations **(***Nat. Nanotechnol.* **15**, 331-341(2020)). As a new kind of nanomedicine, AIE-COFs are postulated to undergo internalization via the canonical endocytosis route, wherein cellular uptake leads to their encapsulation within endosomes. Subsequent maturation and fusion of these endosomes with lysosomes culminate in the sequestration of AIE-COFs within lysosomal compartments. In the future study, we will verify the precise interanimation pathways of AIE COFs.

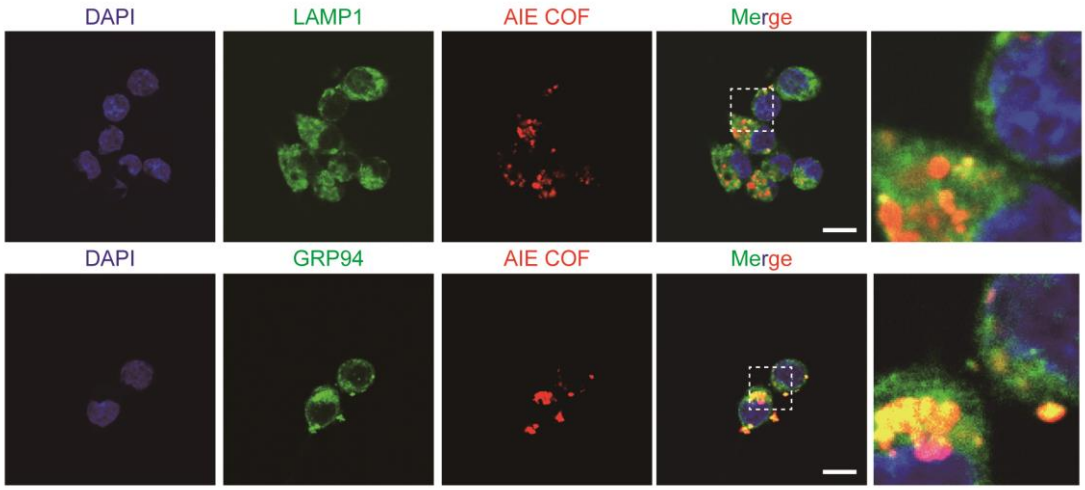

Supplementary Fig. 32. Subcellular distribution of AIE COF in RAW264.7 cell, scale bar = 10 μm.

Comment 4:

4. "*In the revised manuscript, the authors showed the maturation of DCs after treatment with AIE-COFs, in order to show the maturation of DCs more specifically, the authors need to locate DCs by staining the markers of DCs such as CD11C, MHCII. Additionally, it would be more complete if the authors conduct a statistical analysis to the immunostaining images.*"

Response 4:

We sincerely appreciate the reviewer's valuable suggestion regarding the specific identification of dendritic cells (DCs) through markers such as CD11C and MHCII to demonstrate their maturation more clearly. As suggested, we have performed additional immunostaining experiments to specifically locate DCs by staining for CD11C and MHCII. These new experiments confirm the maturation of DCs after treatment with AIE-COFs, and the corresponding results have been included in the revised manuscript Fig. 7e.

Additionally, as recommended by the reviewer, we have conducted a statistical analysis of the immunostaining images to quantify the levels of CD3, CD4, CD19, F4/80, PNAD, CXCL13, $CD11C^{+}MHCII^{+}$, $CD19^{+}CD86^{+}$ and $F4/80^{+}$ $CD86^{+}$ cells. The results, along with statistical annotations, are now presented in the revised Supplementary Fig. 33 to 35 to ensure robust data interpretation.

Revision made:

In the revised manuscript, we labeled the maturation DCs in the tertiary lymphoid structure areas using a CD11C and MHCII antibody with details as following:

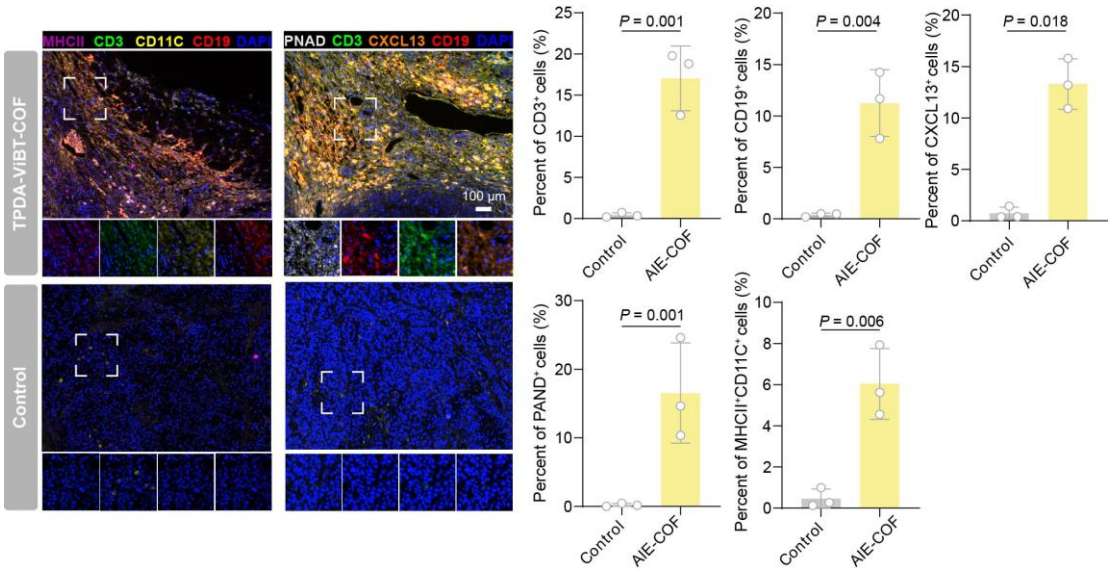

Fig 7e. Representative images and quantification of mIHC staining of MHCII (purple), CD3 (green), CD11C (yellow), CD19 (red), PNAD (white), CXCL13 (orange), and DAPI (blue) in 4MOSC1 tumor with or without TPDA-ViBT-COF treatment, scale bar = 100 μm.

<u>At the same time, we have also performed statistical analysis on the immunostaining images:</u>

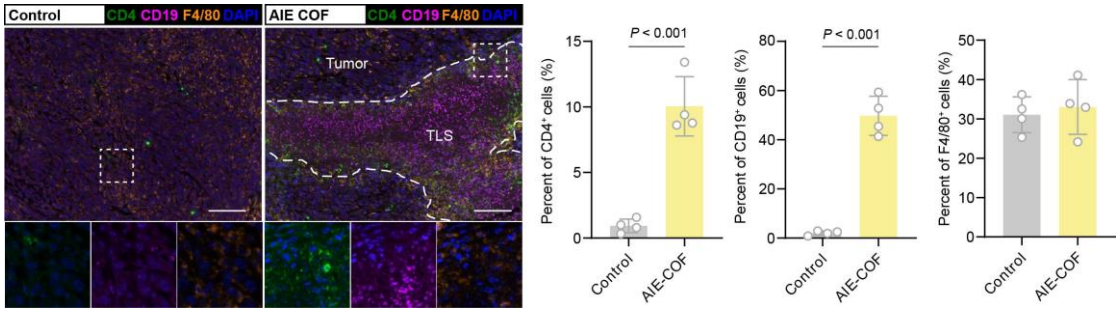

Supplementary Fig. 33. Representative images and quantification of mIHC staining of CD4 (green), CD19 (magenta), F4/80 (yellow), and DAPI (blue) in MC38 tumor after and before TPDA-ViBT-COF treatment, scale bar: 50 μm.

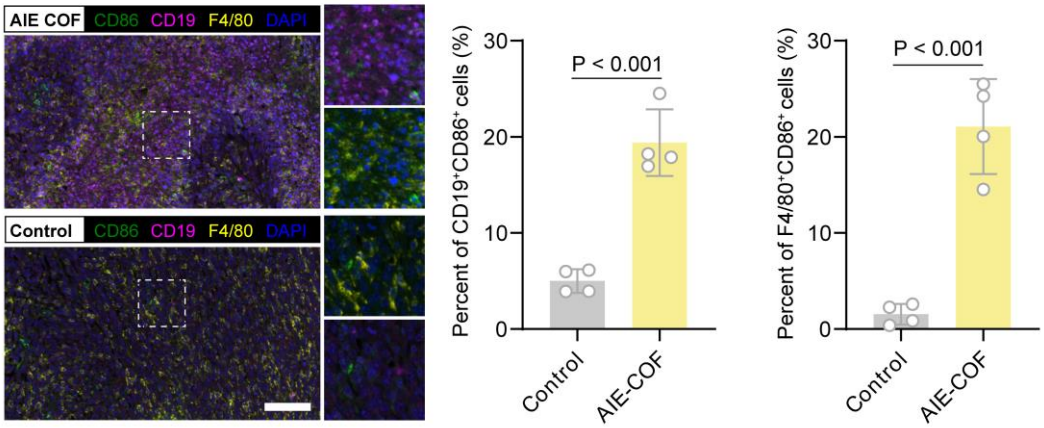

Supplementary Fig. 34. Representative multiplexed immunohistochemical staining images and quantification of CD86 (green), CD19 (magenta), F4/80 (yellow), and DAPI (blue) in MC38 tumor samples that underwent treatment with either control or AIE COF, scale bar: 50 μm.

Point-by-Point Response to Reviewers 3 Comments

Comments:

The re-submitted manuscript entitled "Trigger inducible tertiary lymphoid structure formation using covalent organic frameworks for cancer immunotherapy" have addressed the comments from me and other reviewers comprehensively. The details as well as the organization of data are well improved. However, I still have a few additional concerns as below:

Response:

We are very grateful to the reviewer for pointing out the novelty of our work. We also highly appreciate the reviewer's careful reading and constructive suggestions that helped us to further the quality. By responding to the reviewer's comments in detail and revising the manuscript accordingly, we believe our manuscript has been significantly strengthened. All revisions are highlighted in BLUE color in the revised manuscript and Supplementary Information.

Comment 1:

1. *"The captions of supplementary data are need to be clarified with more detail, such as supplementary figure. 7,30,31."*

Response 1:

We appreciate the reviewer's insightful comment regarding the captions of supplementary data. In response to the reviewer's suggestion, we have added the more detail in supplementary figure. 7, 30, and 31 to ensure that the results are more clearly indicated. Thank you again for your valuable insights. Relevant description has been added to each figure caption with details as the following:

"**Supplementary Fig. 7.** PL spectra of M-TPDA (A), M-TDTA (C), M-BT (E) and M-ViBT (G) in THF/H_2O solutions with different water fractions (f_w). Plots of the relative emission intensity (I/I_0) of M-TPDA (B), M-TDTA (D), M-BT (F) and M-ViBT (H) versus increased water fraction. Source data are provided as a Source Data file.

"**Supplementary Fig. 30.** Representative images of mIHC staining of CD19 (red), CD3 (green), PNAD (white), CD11C (yellow), and DAPI (blue) in TPDA-ViBT-COF treated 4MOSC1 tumor. The images at the bottom show the expression of each single marker assessed, with T cells marker (CD3), B cells marker (CD19), high endothelial venules marker (PNAD), and dendritic cell marker (CD11c), scale bar = 100 μm."

"**Supplementary Fig. 31.** Representative images of mIHC staining of CD19 (red), CD3 (green), PNAD (white), CD11C (yellow), and DAPI (blue) in TPDA-ViBT-COF treated 4MOSC1 tumor. The images at the bottom show the expression of each single marker assessed, with T cells marker (CD3), B cells marker (CD19), high endothelial venules marker (PNAD), and dendritic cell marker (CD11c), scale bar = 100 μm."

Comment 2:

1. "*The details on the statistical analysis of figures and supplementary figures in the captions are further needed to be checked throughout the whole manuscript, such as figure 6f, figure 7c, supplementary figure. 15,16,21 as well as 22.*"

Response 2:

We sincerely thank the reviewer for their careful reading and valuable suggestions. We have thoroughly checked the statistical analysis of figures and supplementary figures. Additionally, we have revised the details about figure captions of 6f, figure 7c, supplementary figure. 15, 16, 21 and 22. Relevant description has been added to each figure caption with details as the following:

"**Figure 6.** (**f)** Quantification of the levels of various cytokines and chemokines in tumors following treatment with control or TPDA-ViBT-COF, n = 5 independent samples, data are presented as mean ± SEM and statistical significance was assessed using two-tailed Student's t-test."

"**Figure 7.** (b) The images and the weight of 4MOSC1 tumors on day 15. Tumor volume **(c)** and body weight (d) of 4MOSC1 tumor-bearing mice, n = 5 independent samples. Data are presented as mean ± SEM, one-way ANOVA with post hoc Tukey test was used when comparing more than two groups. Source data are provided as a Source Data file."

"Supplementary Fig. 15. Quantification and representative immunohistochemical images of Ki67, Cleaved Caspase-3, and Calreticulin under different treatments, scale bar = 50 μm, n = 3 independent samples. Data are presented as mean ± SEM, statistical significance was assessed using one-way ANOVA with post hoc Tukey test. Source data are provided as a Source Data file."

"Supplementary Fig. 16. ATP (A) andLDH (B) in MC38 cells after various treatments; data are presented as mean ± SEM (n = 3 independent samples), statistical significance was assessed using one-way ANOVA with post hoc Tukey test. C, Representative images of HMGB1 immunofluorescence staining in MC38 cells after treatment with different samples. Source data are provided as a Source Data file, scale bar = 50 μm."

"**Supplementary Fig. 21**. (A) Quantification of T cell ($CD3^+$) gating on $CD45^+$ cells in TDLNs, n = 6 independent samples. (B) to (C) Quantification of T cell ($CD3^+$) gating on $CD45^+$ cells in Spleen, n = 6 independent samples. Quantification of MDSC ($Ly6G^{high}$ $Ly6C^{low}$) gating on $CD11b^+$ $MHCII^-$ cells in the spleen, n = 6 independent samples. Data are presented as mean ± SEM, statistical significance was assessed using one-way ANOVA with post hoc Tukey test. Source data are provided as a Source Data file."

"**Supplementary Fig. 22.** Quantification of mIHC staining of CD4 (green), CD19 (magenta), F4/80 (yellow), and DAPI (blue) in MC38 tumor after and before TPDA-ViBT-COF treatment, n = 4 independent samples. Data are presented as mean ± SEM, statistical significance was assessed using two-tailed Student's t-test. Source data are provided as a Source Data file."